Plant Physiology Preview. Published on April 4, 2019, as DOI:10.1104/pp.19.00139

Short title: Polar Auxin Transport during Leaf Thermonasty

Corresponding author: cmpark@snu.ac.kr

Title: Developmental Programming of Thermonastic Leaf Movement

Young-Joon Park,[a] Hyo-Jun Lee,[a,*] Kyung-Eun Gil,[a] Jae Young Kim,[a] June-Hee Lee,[a] Hyodong Lee,[b] Hyung-Taeg Cho,[b] Lam Dai Vu,[c,d,e,f] Ive De Smet,[c,d] and Chung-Mo Park[a,g,2,3]

[a]Department of Chemistry, Seoul National University, Seoul 08826, Korea

[b]Department of Biological Sciences, Seoul National University, Seoul 08826, Korea

[c]Department of Plant Biotechnology and Bioinformatics, Ghent University, B-9052 Ghent, Belgium

[d]VIB Center for Plant Systems Biology, B-9052 Ghent, Belgium

[e]Department of Biomolecular Medicine, Ghent University, B-9000 Ghent, Belgium

[f]VIB Center for Medical Biotechnology, B-9000 Ghent, Belgium

[g]Plant Genomics and Breeding Institute, Seoul National University, Seoul 08826, Korea

One-sentence summary: The developmentally programmed polarity of the auxin response underlies thermo-induced leaf hyponasty

Author contributions: C.-M.P. and Y.-J.P. conceived and designed the experiments. C.-M.P prepared the manuscript with the contributions of Y.-J.P. and H.-J.L. H.-J.L. and Y.-J.P. analyzed hyponasty phenotype, gene expression, ChIP, and thermography. K.-E.G.,J.Y.K., and J.-H.L managed plant growth and provided scientific discussion. H.L. and H.-T.C. contributed to the production of vector constructs and transgenic plants. L.D.V. and I.D.S. provided

scientific discussion.

Responsibilities of the Author for Contact: The author responsible for distribution of materials integral to the findings presented in this article in accordance with the policy described in the Instructions for Authors (www.plantphysiol.org) is: Chung-Mo Park (cmpark@snu.ac.kr).

Funding information: This work was supported by the Leaping Research Program (NRF-2018R1A2A1A19020840) provided by the National Research Foundation of Korea (NRF) and the Next-Generation BioGreen 21 Program (PJ013134) provided by the Rural Development Administration of Korea. Y.-J.P. was partially supported by the Global Ph.D. Fellowship Program through NRF (NRF-2016H1A2A1906534).

*Present address: Korea Research Institute of Bioscience and Biotechnology, Daejeon 34141, Korea

[2]Corresponding author: cmpark@snu.ac.kr

ABSTRACT

Plants exhibit diverse polar behaviors in response to directional and non-directional environmental signals, termed tropic and nastic movements, respectively. The ways in which plants incorporate directional information into tropic behaviors is well understood, but it is less well understood how non-directional stimuli, such as ambient temperatures, specify the polarity of nastic behaviors. Here, we demonstrate that a developmentally programmed polarity of auxin flow underlies thermo-induced leaf hyponasty in Arabidopsis (*Arabidopsis thaliana*). In warm environments, PHYTOCHROME-INTERACTING FACTOR 4 (PIF4) stimulates auxin production in the leaf. This results in the accumulation of auxin in leaf

petioles, where PIF4 directly activates a gene encoding the PINOID (PID) protein kinase. PID is involved in polarization of the auxin transporter PIN-FORMED 3 to the outer membranes of petiole cells. Notably, the leaf polarity-determining ASYMMETRIC LEAVES 1 (AS1) directs the induction of *PID* to occur predominantly in the abaxial petiole region. These observations indicate that the integration of PIF4-mediated auxin biosynthesis and polar transport, and the AS1-mediated developmental shaping of polar auxin flow, coordinate leaf thermonasty, which facilitates leaf cooling in warm environments. We believe that leaf thermonasty is a suitable model system for studying the developmental programming of environmental adaptation in plants.

INTRODUCTION

Plants actively adjust their growth and architecture to adapt to changing environments, in which the roles of auxin are extensively studied. Both biosynthesis and cellular and organismal distribution of auxin are critical for its function (Petrásek and Friml, 2009; Zhao, 2010; Huang et al., 2017). In particular, it is known that polar flow of auxin produces its gradients in different plant tissues, leading to asymmetric cell elongation (Ding et al., 2011). Molecular events leading to polar auxin transport are fairly well understood in terms of the tropic behaviors of plant organs, which occur in response to directional stimuli, such as light and gravity (Ding et al., 2011; Rakusová et al., 2011).

Vesicle-to-membrane trafficking of the auxin efflux transporter PIN-FORMED 3 (PIN3) determines the polarity of auxin flow (Friml et al., 2002; Ding et al., 2011). It has been reported that localized distribution of PIN proteins at different sides of the cell is regulated by developmental pathways and environmental stimuli (Friml et al., 2002; Zádníková et al., 2010). Under unilateral light conditions, PIN3 is localized to the inner membranes of hypocotyl cells on the illuminated side, while it moves to both the inner and outer membranes of hypocotyl cells at the shaded side (Ding et al., 2011; Rakusová et al., 2011). Accordingly,

auxin accumulates in the shaded side, resulting in hypocotyl bending toward light. The polar movement of PIN3 is also important for the gravitropic responses of hypocotyls. It is known that PIN3 is polarized to the outer membranes of hypocotyl cells at the lower side, in response to gravity stimuli (Rakusová et al., 2011).

PINOID (PID) is a protein kinase that is known to phosphorylate PIN3 (Ding et al., 2011). Functional significance of the PID-mediated PIN phosphorylation has been explored (Kleine-Vehn et al., 2009; Zourelidou et al., 2014). It is known that PID-dependent phosphorylation of PIN proteins regulates their polarity (Kleine-Vehn et al., 2009). It also activates the PIN-mediated auxin efflux (Zourelidou et al., 2014). However, the conventional model depicting the PID-mediated regulation of PIN3 polarization through protein phosphorylation might be over-simplified (Weller et al., 2017). It has been suggested that, in addition to the PID-mediated protein phosphorylation, transcriptional regulation of *PIN3* gene, its protein turnover, and as-yet unidentified cellular trafficking systems would also contribute to the PIN3-mediated polar auxin distribution (Willige et al., 2011; Wang et al., 2015; Weller et al., 2017).

There is another type of plant movement responses, termed nastic movements, in which non-directional stimuli, such as temperature, light irradiance, and flooding, trigger directional movements of specific plant organs (Forterre et al., 2005; van Zanten et al., 2009; Keuskamp et al., 2010; Sasidharan et al., 2015). Unlike tropic movements, nastic movements are not affected by the direction of stimuli but instead modulated by the quality of stimuli (Forterre et al., 2005). A well-known example is leaf hyponasty, in which non-directional warm temperature signals stimulate the upward bending of leaf petioles (Koini et al., 2009; van Zanten et al., 2009). The thermally induced nastic leaf behaviors are often termed leaf thermonasty and suggested to play a role in protecting the thermolabile tissues from the radiant heat of the soil surface (Crawford et al., 2012). However, it is unknown how non-directional temperature signals drive directional leaf movement.

105 In plants, it has been suggested that the direction of nastic movements is established
106 by certain developmental programs, which determine the polarity of organ patterning (Nick
107 and Schafer, 1989; Polko et al., 2011). In recent years, the molecular mechanisms and
108 signaling schemes specifying leaf polarity have been studied extensively. The adaxial–abaxial
109 polarity of leaves is determined through complicated signaling networks comprising several
110 proteins and RNA molecules (Kerstetter et al., 2001; Iwasaki et al., 2013; Merelo et al., 2016).
111 The Arabidopsis (*Arabidopsis thaliana*) epigenetic repressors ASYMMETRIC LEAVES 1
112 (AS1) and AS2 act as major upstream regulators of the leaf polarity-determining genes
113 (Iwasaki et al., 2013). They are also required for the polar distribution of auxin at the leaf tip
114 to promote asymmetric differentiation (Zgurski et al., 2005), further supporting the role of AS
115 proteins in specifying the polarity of plant organs.
116 In this work, we demonstrated that hyponastic leaf movement at warm temperatures
117 is modulated by a developmentally programmed auxin gradient in the petiole. Thermo-
118 activated PHYTOCHROME-INTERACTING FACTOR 4 (PIF4) induces *PID* gene, which is
119 known to regulate the auxin transporter PIN3. Notably, PIF4 preferentially binds to the *PID*
120 promoter primarily in the abaxial petiole region at 28°C. Auxin produced via the PIF4-
121 YUCCA8 (YUC8) pathway in the leaf is transported to the petiole and distributed toward the
122 abaxial side of petioles via the polarized action of PID. We conclude that the PIF4-mediated
123 auxin biosynthesis and polar transport and the AS1-directed acceleration of *PID* expression in
124 the abaxial petiole region constitute a thermal pathway that triggers the upward bending of
125 leaf petioles in response to non-directional warm temperature signals. We also found that
126 PIF4-governed leaf thermonasty enhances leaf cooling under warm temperature conditions, as
127 has been shown previously (Crawford et al., 2012).
128
129

RESULTS

Polarization of Leaf Thermonasty Is Independent of Light Direction and Gravity

The leaves of many plant species bend upward at warm temperatures (Lippincott and Lippincott, 2009; van Zanten et al., 2009). Kinetic analysis of *Arabidopsis* petiole bending revealed that the hyponastic response was rapidly initiated within several hours following exposure to 28°C (Figure 1A). We then asked how directional leaf movement occurs in response to ambient temperatures, typical of non-directional environmental signals.

We suspected that the polarity of leaf thermonasty might be influenced by directional environmental cues. Infrared thermography showed that temperatures on the adaxial and abaxial surfaces of leaf blades and petioles were identical during temperature treatments (Figure 1B). We next examined the effects of light direction on leaf thermonasty using upward light illumination. While the extent of hyponastic movement was somewhat different from what observed under downward light illumination, its polarity was not altered by upward light illumination (Figure 1, C and D). Gravity is another unilateral cue (Rakusová et al., 2011). We were not able to detect any effects of horizontal gravitropic stimulation on the polarity of leaf thermonasty (Figure 1, E and F). These observations show that the polarity of leaf thermonasty is not influenced by light direction and gravity.

Auxin Biosynthesis and its Polar Transport Mediate Leaf Thermonasty

The plant growth hormone auxin has been reported to be tightly associated with thermomorphogenesis (Gray et al., 1998; Franklin et al., 2011; Park et al., 2017). To investigate the potential linkage between leaf thermonasty and auxin, we examined localized expression patterns of auxin-responsive genes encoding SMALL AUXIN UP RNA 19 (SAUR19) and SAUR22, in the abaxial and adaxial halves of leaf petioles at 28°C (Supplemental Figure S1A). Thermal induction of *SAUR* genes was larger in the abaxial samples compared to that in the adaxial samples (Figure 2A). In addition, a mutation in the

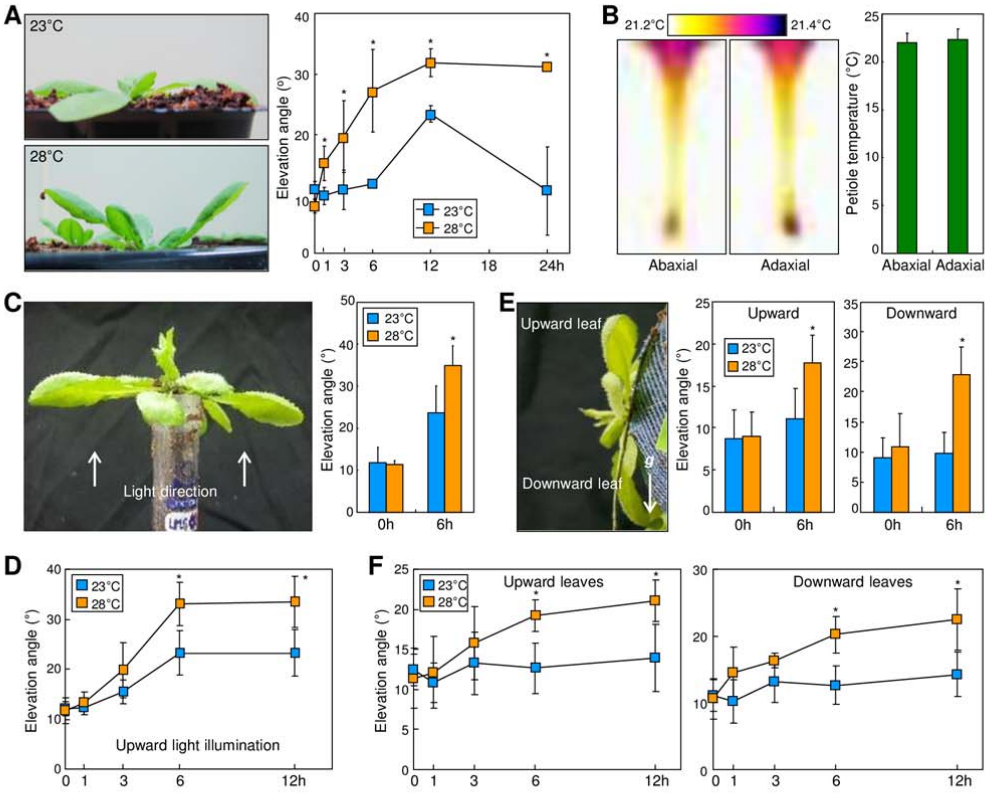

Figure 1. Polarization of leaf thermonasty is independent of light direction and gravity. Elevation angles of the 5th and 6th rosette leaves relative to the horizontal plane were measured using three-week-old plants exposed to 28˚C. Three independent measurements, each consisting of 16 individual plants grown under identical conditions, were statistically analyzed using Student's *t*-test (*$P < 0.01$, difference from 23˚C). Error bars indicate standard error of the mean (SE). h, hour. A, Kinetic effects of warm temperatures on petiole bending. Elevation angles were measured in a time course following exposure to 28˚C. B, Leaf petiole temperatures. Temperatures on the abaxial and adaxial surfaces of leaf petioles were measured by infrared thermography 6 h following exposure to 28˚C. C, Effects of light direction on leaf thermonasty. Plants were exposed to 28˚C for 6 h with upward light illumination. D, Kinetic effects of warm temperatures and light directions on petiole bending. Elevation angles were measured in a time course following exposure to 28˚C with upward light illumination. E, Effects of gravity on leaf thermonasty. Plants were subjected to horizontal gravitropic stimulation (*g*) at 28˚C for 6 h in the light. F, Kinetic effects of warm temperatures and gravity on petiole bending. Elevation angles were measured in a time course following exposure to 28˚C with horizontal gravitropic stimulation, as depicted in (E).

gene encoding the auxin receptor TRANSPORT INHIBITOR RESPONSE 1 (TIR1) caused reduced thermonastic leaf bending (Figure 2B). These observations suggest that auxin is involved in the thermal regulation of leaf hyponasty.

To investigate the association between polar auxin accumulation and leaf thermonasty, we employed the DR5:GUS auxin reporter plants. Gene expression analysis revealed that the expression of the *β-glucuronidase* (*GUS*) reporter gene was elevated by ~2-fold in the abaxial

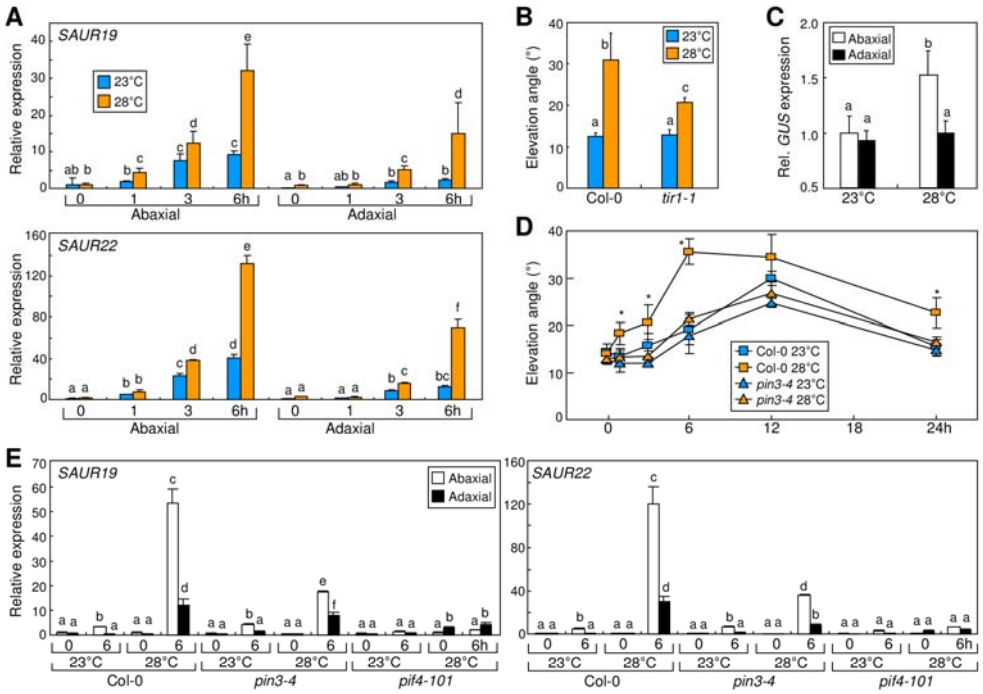

Figure 2. Expression of auxin response genes is elevated in the abaxial petiole region during leaf thermonasty. Three independent measurements, each consisting of 16 individual plants grown under identical conditions, were subjected to statistical analysis. Different letters represent a significant difference ($P < 0.01$) determined by one-way analysis of variance with *post hoc* Tukey test. Error bars indicate SE. A, Transcription of *SMALL AUXIN UP RNA* (*SAUR*) genes. Three-week-old Col-0 plants were exposed to 28˚C before preparing dissected petiole samples for total RNA extraction. Transcript levels were analyzed by RT-qPCR. B, Leaf thermonasty in *tir1-1* mutant. Plants were temperature-treated as described above. C, Transcription of *glucuronidase* (*GUS*) reporter. The DR5:GUS plants were exposed to 28˚C for 6 h, and petiole sampling and RT-qPCR were performed as described above. D, Leaf thermonasty in *pin3-4* mutant. Statistical analysis was performed using Student's *t*-test (*$P < 0.01$, difference from 23˚C). E, Transcription of *SAUR* genes in *pin3-4* and *pif4-101* mutants. Temperature treatments, preparation of petiole samples, and RT-qPCR were performed as described above.

petiole region but was not discernibly altered in the adaxial petiole region in 28°C-treated plants (Figure 2C). Utilization of the fluorescent auxin system, the DII-VENUS reporter, revealed that fluorescence intensity was significantly lower in the abaxial epidermal regions than in adaxial epidermal regions at 28°C (Supplemental Figure S1B). Consistent with this, inhibition of auxin transport by 1-N-Naphthylphthalamic acid (NPA) significantly abolished leaf thermonasty (Supplemental Figure S2A). In addition, exogenous application of indole acetic acid (IAA) to the adaxial petiole region significantly reduced leaf elevation at warm temperatures (Supplemental Figure S2B). These data suggest that preferential auxin accumulation in the abaxial petiole region is closely linked with leaf thermonasty.

Meanwhile, it is well-known that warm temperatures trigger auxin biosynthesis through the PIF4-mediated induction of *YUC8* gene (Gray et al., 1998; Franklin et al., 2011; Park et al., 2017), raising a possibility that the PIF4-mediated auxin biosynthesis would be functionally associated with leaf thermonasty. We first examined whether thermal induction of leaf elevation occur in *yuc8* mutant. As anticipated, leaf thermonastic movement was largely impaired in the mutant (Supplemental Figure S2C). In addition, pretreatments with yucasin, a potent inhibitor of YUC enzymes (Nishimura et al., 2014), abolished leaf thermonasty in Col-0 plants (Supplemental Figure S2D), supporting that thermo-induced auxin biosynthesis is required for leaf thermonasty. Auxin is produced mainly in leaf blade in response to environmental stimuli (Michaud et al., 2017). Accordingly, when leaf blade was excised, upward petiole bending did not occur at warm temperatures (Supplemental Figure S2E). In addition, the thermal induction of *YUC8* expression was only marginal in the leaf petioles (Supplemental Figure S2F), further supporting the notion that auxin biosynthesis occurs mainly in leaf blade. Taken together, these observations clearly show that both auxin biosynthesis and its polar transport are important for leaf thermonasty.

On the basis of the functional association between polar auxin transport and leaf hyponasty (Pantazopoulou et al., 2017), we examined any potential roles of the PIN3 transporter during leaf thermonasty. Notably, leaf thermonasty did not occur in the PIN3-deficient *pin3-4* mutant (Figure 2D), consistent with the reduced thermal induction of *SAUR* genes in the *pin3-4* mutant (Figure 2E). Thermal induction of *SAUR* genes was also compromised in the *pif4-101* mutant, which exhibits disturbed leaf thermonasty (Koini et al., 2009). These observations support that PIN3-mediated polar auxin transport is critical for leaf thermonasty.

PID is Associated with Leaf Thermonasty

Cellular functions of PIN proteins are regulated at multiple levels, such as gene transcription,

intracellular trafficking, and protein stability (Willige et al., 2011; Wang et al., 2015; Weller et al., 2017). Gene expression analysis using dissected leaf petiole samples revealed that the transcription of *PIN3* gene was elevated more than 2-fold in both the abaxial and adaxial sides at 28°C (Supplemental Figure S3A). Since thermal induction of *PIN3* expression occurs in both sides of the petioles, other regulatory mechanisms rather than transcriptional control would play a major role in regulating the asymmetric PIN3 function during leaf thermonasty.

Intracellular distribution of PIN3 is a critical event in establishing polar auxin flow (Ding *et al.,* 2011; Rakusová *et al.,* 2011). To investigate whether intracellular distribution of PIN3 is associated with leaf thermonasty, we expressed a *PIN3-Green Fluorescence Protein* (*GFP*) gene fusion driven by the endogenous *PIN3* promoter in Col-0 plants, and the distribution patterns of GFP signals were examined in the leaf petiole cells. It is known that PIN3 is produced mainly in the endodermal cells of the shoots, which are a major barrier of auxin flow between vasculature and outer cell layers (Ding *et al.,* 2011). Considering the notion that chlorophyll autofluorescence is relatively weaker in the endodermal cells compared to that in the epidermal cells (Keuskamp *et al.,* 2010), we identified the endodermal cells for the examination of the intracellular distribution of PIN3-GFP proteins.

At 23°C, the PIN3 proteins were distributed equally in the outer membranes of both adaxial and abaxial petiole cells (Figure 3, A and B and Supplemental Figure S3B). In contrast, at 28°C, more PIN3 proteins were localized in the outer membranes of abaxial petiole cells than adaxial petiole cells, indicating that warm temperatures stimulate the polarization of PIN3 to the outer membranes of the abaxial petiole cells. It is known that polar PIN3 localization under unilateral light or gravity stimulation is efficiently blocked by brefeldin A (BFA), a potent inhibitor of vesicle trafficking (Ding *et al.,* 2011, Weller *et al.,* 2017). We found that leaf thermonasty was discernibly suppressed in the presence of BFA (Figure 3C). Polarization of PIN3 to the abaxial petiole cells was also blocked by BFA treatments in warm temperature conditions (Supplemental Figure S4, A and B). This indicates

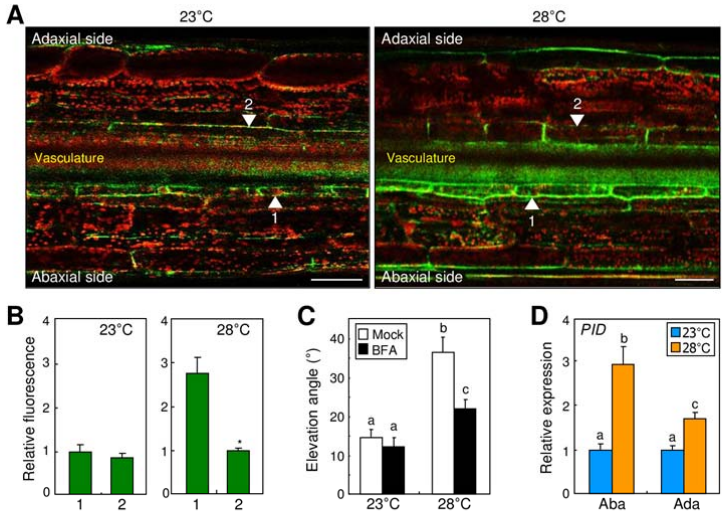

Figure 3. PIN3 is polarized to the outer membranes of abaxial endodermal cells in leaf petioles at warm temperatures. Three independent measurements, each consisting of 8 individual plants grown under identical conditions, were statistically analyzed. Error bars indicate SE. In (C) and (D), different letters represent a significant difference ($P < 0.01$) determined by one-way analysis of variance with *post hoc* Tukey test. A and B, Polar distribution of PIN-FORMED 3 (PIN3). Three-week-old plants expressing a *PIN3-GFP* fusion driven by the endogenous *PIN3* promoter were exposed to 28˚C for 6 h before fluorescence microscopy of the 5th leaf petioles. Green and red signals indicate PIN3-GFP and chlorophyll autofluorescence, respectively (A). Arrowheads indicate the outer membranes of petiole endodermal cells. Scale bars, 100 μm. PIN3-GFP signals were quantitated (*t*-test, $*P < 0.01$) (B). C, Effects of brefeldin A (BFA) on leaf thermonasty. A 10 μM BFA solution was sprayed on the petioles before exposure to 28˚C. Elevation angles were measured and statistically analyzed. D, Transcription of *PINOID* (*PID*) gene. Leaf petioles of Col-0 plants were dissected into abaxial and adaxial halves. Transcript levels were analyzed by RT-qPCR.

that, during leaf thermonasty, BFA-sensitive vesicular trafficking drives the thermo-induced polarization of PIN3. Intracellular aggregates, termed BFA bodies, are frequently observed in plant cells, mostly root cells, when treated with BFA (Jásik et al., 2016). We did not observe such BFA bodies in our assay conditions, similar to what observed with the fluorescence images of hypocotyl cells (Ding et al., 2011). It is likely that BFA bodies may not be readily visible in all tissue cells.

We next analyzed the transcription of genes encoding regulators of PIN3 polarization at warm temperatures. Notably, the transcription of *PID* and *WAG2* genes, which encode serine/threonine protein kinases that phosphorylate PIN3 (Dhonukshe *et al.,* 2010), was elevated to higher levels in the abaxial petiole cells than in the adaxial petiole cells (Figure 3D

and Supplemental Figure S4C). The transcription of *ARABIDOPSIS* H^+ *ATPase* (*AHA*), *SERINE/THREONINE PROTEIN PHOSPHATASE 2A* (*PP2A*), and *D6 PROTEIN KINASE* (*D6PK*) genes was also elevated slightly in the adaxial petiole regions (Supplemental Figure S4C). Since polar auxin transport is more active in the abaxial petiole regions, it seems likely that altered transcript levels of *AHA*, *PP2A*, and *D6PK* genes play a minor role during leaf thermonasty. Considering that PID function is regulated primarily at the transcriptional level (Ding *et al.,* 2011), we hypothesized that differential production of PID in the abaxial and adaxial petiole cells would be functionally linked with PIN3 polarization at warm temperatures.

To examine the functional linkage between the differential *PID* transcription in petiole cells and leaf thermonasty, we analyzed the effects of warm temperatures on the transcription of auxin-responsive genes in transgenic plants overexpressing *PID* gene driven by the strong cauliflower mosaic virus (CaMV) 35S promoter. Because of the molecular nature of the promoter used, it was thought that differential expression of the *PID* gene in the abaxial and adaxial sides would be disturbed in the transgenic plants. As expected, the polarization patterns of PIN3 to the outer membranes were similar in the abaxial and adaxial petiole cells at both 23°C and 28°C (Figure 4, A and B and Supplemental Figure S5, A and B). Leaf thermonasty was also impaired in the *PID*-overexpressing plants (Figure 4C), and thermal induction of *SAUR22* gene expression was largely reduced in the transgenic plants (Figure 4D), supporting that PID is important for leaf thermonasty.

Leaf thermonasty was also disturbed in the *pid wag1 wag2* triple mutant (Supplemental Fig S5C). However, the phenotype of the triple mutant should be considered with caution because the lack of leaf thermonasty might be attributed to other developmental defects in the mutant. It has been reported that the triple mutant is defective in leaf organogenesis (Dhonukshe et al., 2010). It is known that PID trafficking to the cellular membranes is associated with PIN function (Kleine-Vehn et al., 2009). Transient expression

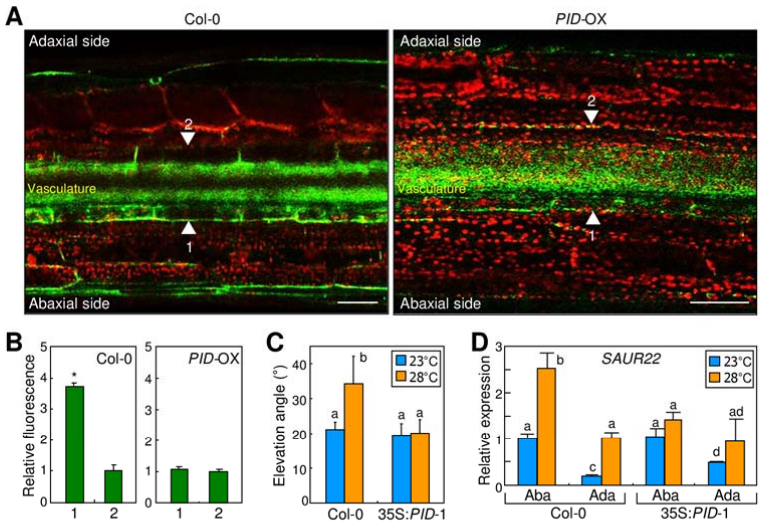

Figure 4. PID-directed PIN3 polarization underlies leaf thermonasty. Three independent measurements, each consisting of 16 individual plants grown under identical conditions, were statistically analyzed. In (C) and (D), different letters represent a significant difference ($P < 0.01$) determined by one-way analysis of variance with *post hoc* Tukey test. Error bars indicate SE. A and B, Polar distribution of PIN3. Three-week-old plants expressing a *PIN3-GFP* fusion driven by the endogenous *PIN3* promoter were exposed to 28˚C for 6 h before fluorescence microscopy of the 5th leaf petioles (A). Arrowheads indicate the outer membranes of petiole endodermal cells. Scale bars, 100 μm. PIN3-GFP signals were quantitated (*t*-test, $*P < 0.01$) (B). (C) Leaf thermonasty in 35S:*PID* plants. (D) Transcription of *SAUR22* gene in 35S:*PID* plants. Leaf petioles were dissected into abaxial and adaxial halves. Transcript levels were analyzed by RT-qPCR.

of the *GFP-PID* fusion in *Arabidopsis* protoplasts revealed that PID proteins are predominantly localized to the membranes at both 23°C and 28°C (Supplemental Figure S5D), which is also consistent with the roles of PID at the cell periphery in the previous report (Kleine-Vehn et al., 2009). Together, these observations indicate that PIN3-mediated polar auxin flow is mediated by PID, which is differentially produced in the abaxial and adaxial petiole cells during leaf thermonasty.

PIF4 Activates *PID* Transcription

A next question was how *PID* transcription is differentiated in the abaxial and adaxial petiole cells at warm temperatures. We found that leaf thermonasty and *SAUR* gene expression were disrupted in the *pif4-101* mutant (Figure 2E; Koini et al., 2009), raising a possibility that PIF4 would regulate *PID* transcription in response to warm temperatures. Gene expression analysis

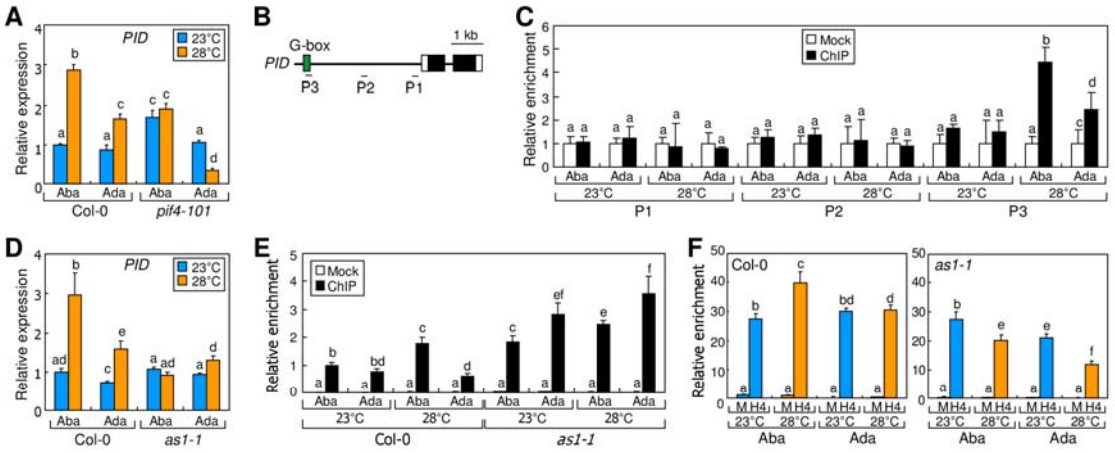

Figure 5. PIF4 and AS1-mediated developmental signals activate *PID* transcription in the abaxial petiole region at warm temperatures. Three independent measurements, each consisting of 16 individual plants grown under identical conditions, were statistically analyzed. Different letters represent a significant difference ($P < 0.01$) determined by one-way analysis of variance with *post hoc* Tukey test. Error bars indicate SE (A and D) or standard deviation of the mean (SD) (C, E, and F). A, *PID* transcription in *pif4-101* mutant. Three-week-old plants were exposed to 28˚C for 6 h. Transcript levels were analyzed by RT-qPCR. B, Genomic structure of *PID* locus. Black boxes are exons, and white boxes are 5' and 3' untranslated regions. The P1 - P3 sequences were analyzed in chromatin immunoprecipitation (ChIP) assays. C, PHYTOCHROME INTERACTING FACTOR 4 (PIF4) binding to *PID* promoter. Three-week-old plants expressing a *PIF4-FLAG* fusion driven by the endogenous *PIF4* promoter were exposed to 28˚C for 6 h. ChIP assays were performed using an anti-FLAG antibody. D, Transcription of *PID* gene in *as1-1* leaf petioles. Transcript levels were analyzed by RT-qPCR. E, PIF4 binding to *PID* promoter in *as1-1* mutant. A *PIF4-FLAG* fusion was expressed driven by the endogenous *PIF4* promoter in Col-0 plants and *as1-1* mutant. The P3 sequence was used in the assay. F, Histone 4 (H4) acetylation in *PID* chromatin. ChIP assays were performed using either Col-0 or *as1-1* leaf petioles. An anti-H4Ac antibody was used for immunoprecipitation. H4 acetylation was analyzed by ChIP-qPCR. M, mock.

revealed that *PID* transcription was somewhat higher in the abaxial petiole cells of *pif4-101* mutant at 23°C (Figure 5A). Notably, thermal induction of *PID* transcription did not occur in the abaxial petiole cells of the mutant. In addition, *PID* transcription was even reduced in the adaxial petiole cells of the mutant at warm temperatures. It seems that additional factor(s), in addition to PIF4, might also be involved in the thermal regulation of *PID* transcription.

To investigate PIF4 binding to *PID* chromatin *in vivo*, we conducted chromatin immunoprecipitation (ChIP) assays using transgenic plants expressing a *PIF4-FLAG* gene fusion driven by the endogenous *PIF4* promoter. While PIF4 binding to *PID* chromatin was not detected at 23°C, PIF4 evidently bound to the P3 sequence region harboring a G-box motif in *PID* chromatin at 28°C (Figure 5, B and C), which is known as the PIF4 binding

motif (Oh et al., 2012). Notably, thermo-induced DNA binding of PIF4 was more prominent in the abaxial petiole cells (Figure 5C), which is in good agreement with the higher induction of *PID* gene in these cells at 28°C.

We next examined PIN3 distribution in the *pif4-101* mutant that expresses a *PIN3-GFP* gene fusion driven by the endogenous *PIN3* promoter. It was found that the thermally induced polarization of PIN3 to the abaxial endodermal cells was not observed in the *pif4-101* mutant (Supplemental Figure S6), indicating that the PIF4 is linked with PIN3 polarization during leaf thermonasty.

AS1 Modulates the PID-mediated Polar Transport of PIN3

A critical issue was how the polarity of leaf thermonasty is established in response to non-directional temperature signals. It has been suggested that hyponastic leaf movement would be related with developmental programs that determine leaf polarity (Nick and Schafer, 1989; Polko et al., 2011). AS1 is the epigenetic repressor that functions upstream of leaf polarity-specifying genes (Zgurski et al., 2005; Iwasaki et al., 2013). Thus, we analyzed possible roles of AS1 during leaf thermonasty. It was revealed that the AS1-deficient *as1-1* mutant did not exhibit any symptoms of leaf thermonasty (Supplemental Figure S7A). Different leaf angles in the mutants at 23°C would be attributed to a developmental disruption of abaxial–adaxial polarity, rather than a constitutive thermomorphogenic response, as has been observed in related mutants exhibiting abnormal leaf polarity (Izhaki et al., 2007; Pérez-Pérez et al., 2010). Consistently, it was found that the thermal induction of *SAUR* and *PID* genes was abolished in the abaxial petiole cells of the *as1-1* mutant (Figure 5D and Supplemental Figure S7B). These observations indicate that AS1 plays a role in modulating PID-mediated auxin response during leaf thermonasty.

It has been reported that AS1 modulates *AUXIN RESPONSE FACTOR3 (ARF3)* expression during the adaxial–abaxial partitioning of a leaf (Iwasaki et al., 2013). In order to

examine whether auxin response is altered in *as1-1* mutant, we analyzed *PID* transcription in leaf petioles treated with IAA. Consistent with the previous report (Bai and Demason, 2008), exogenous application of IAA promoted the *PID* transcription in the leaf petioles of Col-0 plants (Supplemental Figure S7C). In contrast, the inductive effects of IAA disappeared in *tir1* mutant. Notably, the IAA-mediated induction of *PID* transcription still occurred in *as1-1* mutant, suggesting that the *as1-1* mutant retains the capacity of auxin responsiveness in gene expression. On the other hand, polar localization of PIN3 to the outer membranes of the abaxial petiole cells was compromised in the mutant at 28°C (Supplemental Figure S8). It is thus evident that AS1 plays a role in the polar transport of PIN3 during leaf thermonasty.

AS1 Specifies the Polarity of Leaf Thermonasty

A next question was how AS1 modulates *PID* expression in the petiole cells. Yeast two-hybrid assay revealed that AS1 does not interact with PIF4, the regulator of *PID* transcription (Supplemental Figure S7D). In addition, the transcript levels of *PIF4* gene were similar in the petioles of Col-0 plants and *as1-1* mutant (Supplemental Figure S7E). Considering the signaling linkage between PID-mediated auxin response and AS1, we hypothesized that AS1 would modulate the binding of PIF4 to the promoter of *PID* gene at 28°C. ChIP assays revealed that PIF4 binding to the *PID* promoter was more prominent in the abaxial regions than in the adaxial regions of Col-0 leaf petioles at warm temperatures (Figure 5E). In contrast, the DNA binding of PIF4 was higher in the adaxial region of *as1-1* leaf petioles at both 23°C and 28°C (Figure 5E). These observations indicate that the DNA-binding affinity of PIF4 is differentially affected in *as1-1* mutant.

To explore molecular events mediating PIF4 binding to *PID* promoter, we investigated the chromatin modification patterns in the P3 sequence region of *PID* chromatin (Figure 5B). Interestingly, histone 4 (H4) acetylation, an active transcriptional marker (Akhtar and Becker, 2000), was significantly elevated in the abaxial petiole cells but not in the adaxial

333 petiole cells at warm temperatures (Figure 5F). In contrast, the thermal induction of H4
334 acetylation in the P3 sequence was even reduced in the *as1-1* mutant (Figure 5F).

335 We next examined whether the H4 acetylation is functionally important for leaf
336 thermonasty by employing chemical inhibitors of histone deacetylases. Leaf thermonasty was
337 found to be disrupted in Col-0 plants treated with Trichostatin A (TSA) and 4-
338 (dimethylamino)-N-[6-(hydroxyamino)-6-oxohexyl]-benzamide (CAY) (Supplemental Figure
339 S9A), which strongly inhibit histone deacetylases in plants (Ueno et al., 2007 and
340 Supplemental Figure S9B). While the levels of global H4 acetylation were unaltered at warm
341 temperatures (Supplemental Figure S9B), the pattern of H4 acetylation was discernibly
342 altered in the *PID* promoter (Figure 5F), supporting the notion that the thermal regulation of
343 H4 acetylation is specific to the *PID* promoter during leaf thermonasty. Together, these
344 observations illustrate that warm temperatures induce H4 acetylation in the *PID* promoter
345 predominantly in the abaxial petiole cells to facilitate the DNA binding of PIF4.

346

347 **Leaf Thermonasty Lowers Leaf Temperatures**

348 Thermomorphogenic modifications of morphology and architecture are considered to help
349 plants to enhance body cooling capacity by facilitating heat dissipation (Crawford et al., 2012).
350 Leaf thermonasty is a representative thermomorphogenic event occurring at warm
351 temperatures, entailing that it would be functionally associated with leaf cooling capacity.

352 We employed infrared thermography to monitor leaf temperatures under warm
353 temperature conditions. For comparison, the rosette leaves of *pif4-101* mutant were physically
354 lifted so that elevation angles of the mutant leaves were similar to those of Col-0 leaves at
355 warm temperatures (Figure 6A). It was found that leaf temperature was significantly higher in
356 the *pif4-101* mutant compared to that in Col-0 leaves (Figure 6, A and B). Notably, leaf
357 temperatures were similar in Col-0 plants and in the *pif4-101* mutant having physically lifted
358 rosette leaves, supporting that leaf hyponasty is directly related with leaf temperatures.

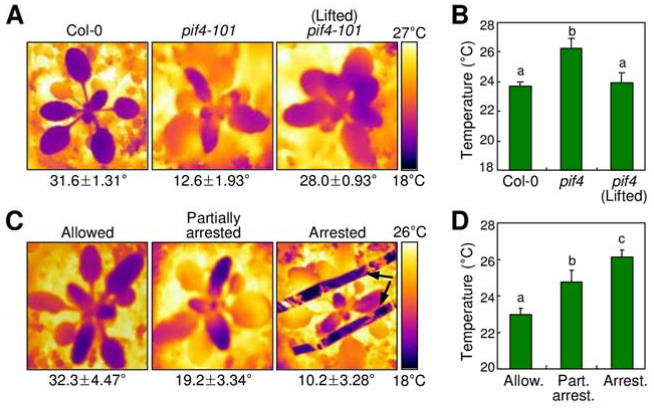

Figure 6. Leaf cooling is associated with hyponastic leaf movement. Three-week-old plants were exposed to 28˚C for 6 h before taking infrared thermographs (left panels). Elevation angles were given below thermographs. Temperatures at the central blade areas of the 6th rosette leaves were measured (right graphs). Three independent measurements, each consisting of 8 individual plants grown under identical conditions, were statistically analyzed. Different letters represent a significant difference ($P < 0.01$) determined by one-way analysis of variance with *post hoc* Tukey test. Error bars indicate SE. A and B, Leaf temperatures in *pif4-101* mutant. For comparison, the mutant rosette leaves were physically lifted to mimic the increased leaf hyponasty as observed in Col-0 plants. C and D, Leaf temperatures in Col-0 plants having physically arrested leaf hyponasty. The rosette leaves were arrested physically to the soil so that leaf hyponasty is not elevated at 28˚C. Arrows marks arresting wires.

359 To further examine the effects of thermonastic leaf movement on leaf cooling, the
360 rosette leaves of Col-0 plants were physically arrested to the soil surface so that the leaves are
361 not able to bend upward at warm temperatures, mimicking those having disrupted
362 thermonastic movement. Leaf cooling was proportional to the elevation angles of rosette
363 leaves (Figure 6, C and D), verifying that leaf hyponasty is critical for leaf cooling under
364 warm environments.

365

366

DISCUSSION

Thermomorphogenesis refers to a suite of plant morphological and architectural modifications, such as hypocotyl elongation, increase of leaf hyponasty, small, thin leaves, and leaf petiole elongation, that occur in response to changes in ambient temperatures (Koini et al., 2009; Franklin et al., 2011; Crawford et al., 2012; Park et al., 2017).

The PIF4 transcription factor, which has been originally identified as a key signaling component of plant photomorphogenesis (Lorrain et al., 2008), plays a central role in warm temperature-mediated morphogenic responses. Accordingly, a wide array of thermomorphogenic responses is impaired in PIF4-defective mutants (Koini et al., 2009). PIF4 directly activates the transcription of *YUC8* gene encoding an auxin biosynthetic enzyme, triggering a complex network of thermal responses (Sun et al., 2012). Recently, it has been reported that BRASSINAZOLE-RESISTANT 1, a transcriptional factor that mediates brassinosteroid signaling (Ryu et al., 2007), is involved in the PIF4-mediated thermomorphogenesis (Ibañez et al., 2018), further extending the complexity of PIF4 signaling.

In this work, we demonstrated that the central thermomorphogenic regulator PIF4 constitutes a distinct, two-branched auxin signaling pathway that modulates hyponastic leaf movement under warm temperature conditions. Thermo-activated PIF4 directly stimulates *PID* transcription in petiole cells, resulting in polar auxin accumulation. In another route, the PIF4-YUC8 branch promotes auxin production in leaf blade, which is transported to the petiole and functions as the substrate for PIN3 machinery. The PIF4-mediated leaf thermonasty also requires AS1-mediated developmental cues that direct PIF4-mediated *PID* transcription to occur mostly in the abaxial petiole region (Figure 7). The working scheme of PIF4 and AS1 in triggering leaf thermonasty illustrates a seminal mode of developmental programming of environmental adaptation, which would also be applicable to other nastic

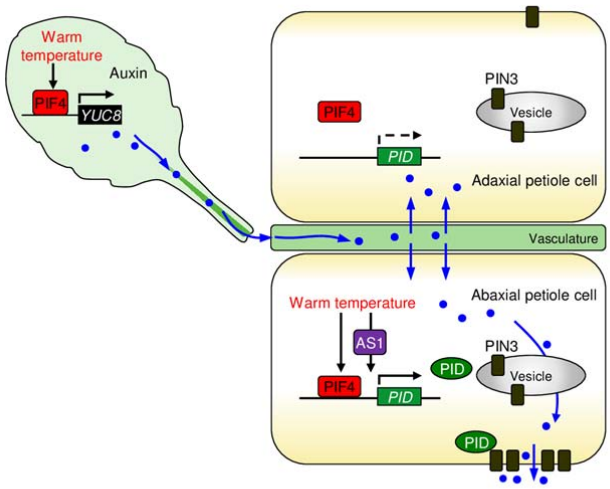

Figure 7. Schematic model for developmental shaping of polar auxin flow during leaf thermonasty. Thermo-activated PIF4 triggers auxin production in the leaf blade. Auxin is then transported to the petiole, where it is distributed toward epidermis via PIN3. PIF4 also activates *PID* transcription in the petiole. The leaf polarity determinant ASYMMETRIC LEAVES 1 (AS1) directs *PID* transcription to occur predominantly in the abaxial petiole region. The PID-mediated PIN3 polarization to the outer membrane of abaxial petiole cells determines the direction of leaf bending. Blue arrows marks the paths of auxin flow.

392 movements in plants.

393 Our observations imply that some additional regulators other than PID might also be
394 involved in the thermal activation of PIN3 during leaf thermonasty. For example, *PID*
395 transcription was differentially regulated in the abaxial and adaxial cells of *pif4-101* mutant,
396 while PIN3 proteins were equally distributed in the petiole cells. In addition, gene expression
397 analysis showed that some additional transcriptional regulators other than PIF4 might be
398 linked with the transcription of *PID*. It was also found that exogenous application of auxin
399 induced *PID* transcription, consistent with the previous report (Bai and Demason, 2008),
400 further supporting the notion that *PID* transcription is modulated by multiple factors. It is
401 probable that auxin-responsive transcription factors, including ARFs, would contribute to *PID*
402 transcription, directly or indirectly, during leaf thermonasty.

403 It is notable that the leaf polarity-specifying AS1 incorporates developmental cues
404 into *PID* expression. AS1 specifies the polarity of lateral organs, in particular, rosette leaves in

405 *Arabidopsis* (Zgurski et al., 2005; Iwasaki et al., 2013). It was observed that H4 acetylation in
406 *PID* chromatin and the binding of PIF4 to *PID* chromatin were discernibly affected in *as1-1*
407 mutant. However, interpretation of thermomorphogenic phenotypes and biochemical events in
408 *as1-1* should be considered with caution in that *as1-1* mutant might exhibit stunted growth
409 and pleiotropic effects caused by distorted leaf polarity. It is currently unclear whether the
410 alterations in DNA binding of PIF4 and H4 acetylation in *PID* chromatin of *as1-1* mutant are
411 functionally inter-related or not. In addition, while PIF4 binds to the *PID* promoter
412 irrespective of the *as1-1* mutation, the thermal induction of *PID* expression was impaired in
413 the mutant. Thus, it remains to be elucidated whether and how AS1 collaborates with PIF4 in
414 inducing *PID* transcription during leaf thermonasty.

415 Our observations demonstrate that the PIN3-mediated polar auxin transport
416 constitutes an important biochemical event during leaf thermonasty. It is notable that PIN
417 proteins are intimately associated with directional movements of plant organs. Especially,
418 PIN3, PIN4 and PIN7 proteins are required for the gravitropic and phototropic responses of
419 hypocotyls (Ding et al., 2011; Rakusová et al., 2011). Meanwhile, PIN2 protein contributes to
420 root gravitropism (Rahman et al., 2010). It is possible that multiple PIN proteins are
421 modulated by diverse environmental stimuli, such as ambient temperature, gravity, and
422 unilateral light, in order to optimize auxin distribution in different plant organs. It will be
423 interesting to examine whether PIN members other than PIN3 are also functionally associated
424 with leaf thermonasty.

425 Our data define a distinct signaling network that mediates the developmental shaping
426 of a hyponastic response occurring in leaf petioles at warm temperatures. It is evident that the
427 polarity of leaf thermonasty is not determined by temperature differences and directional light
428 and gravity stimuli but instead established by the AS1-mediated developmental program.
429 Plants exhibit various types of nastic movements (Forterre et al., 2005; van Zanten et al., 2009;

Sasidharan et al., 2015). In mimosa and Venus flytrap, simple touching promotes water transport to the specific sites of plant organs, resulting in rapid and directional nastic movements (Forterre et al., 2005). In *Arabidopsis*, flooding triggers ethylene accumulation and asymmetric growth in leaf petioles, causing upward hyponastic bending (Sasidharan et al., 2015). It is worthy of investigating whether AS1 is also involved in these nastic movements in plants.

MATERIALS AND METHODS

Plant Materials and Culture Conditions

All Arabidopsis (*Arabidopsis thaliana*) lines used were in Columbia (Col-0) background. The *pin3-4* (SALK-038609), *as1-1* (CS146), *yuc8* (SALK-096110), and *tir1-1* (CS3798) mutants were obtained from a pool of mutant lines deposited in the Arabidopsis Biological Resource Center (Ohio State University, OH). The *pif4-101* mutant (Garlic-114-G06) has been described previously (Lorrain et al., 2008). The DII-VENUS plants were obtained from Jae-Yean Kim. The *pid wag1 wag2* triple mutant was obtained from Remko Offringa (Dhonukshe et al., 2010).

Expression vectors harboring the p*PIN3:PIN3-GFP* gene fusions have been described previously (Ganguly *et al.,* 2012). The expression vectors were transformed into *pif4-101* and *as1-1* mutants (Supplemental Figure S10). To generate 35S:*PID* transgenic plants, a PID-coding sequence was amplified from Col-0 cDNA using a pair of primers: MYC-PID F (ACCCGGGTTATGTTACGAGAATCAGACGGT) and MYC-PID R (AATGGATCCTCAAAAGTAATCGAACGCCG), with XmaI and BamHI sites, respectively. The amplified PCR products were fused in-frame to the 5′ end of a MYC-coding sequence in the myc-PBA vector. The vector construct was then transformed into

transgenic plants expressing the p*PIN3:PIN3-GFP* fusion in Col-0 background. The p*PIF4:PIF4-FLAG* transgenic plants were generated by transforming the p*PIF4:PIF4-FLAG*-containing vector, which has been described previously (Lee et al., 2014), into *as1-1* mutant.

Sterilized Arabidopsis seeds were cold-imbibed at 4°C for 3 d in complete darkness and allowed to germinate either in soil or on ½ X Murashige and Skoog-agar (MS-agar) plates under long days (16-h light and 8-h dark) with white light illumination (120 μmol $m^{-2}s^{-1}$) provided by fluorescent FLR40D/A tubes (Osram, Seoul, Korea) in a controlled growth chamber set at 23°C. Three-week-old plants were subjected to temperature treatments at zeitgeber time 2 (ZT2) for 6 h, unless otherwise mentioned.

Measurement of Leaf Angles

Leaf hyponasty was analyzed using digital images of three-week-old plants exposed to different temperatures at ZT2. Leaf angles were measured at ZT 8 otherwise mentioned. Quantification of elevation angles was performed using the ImageJ software (http://imagej.nih.gov/ij/).

Infrared Thermography

Thermal images of three-week-old plants were recorded using the thermal imaging camera T420 (FLIR, Wilsonville, OR). The thermal images were analyzed using the FLIR Tools (http://www.flirkorea.com/home/), and leaf temperatures were recorded in the central area of the 6^{th} rosette leaves.

Sample Preparation for Abaxial and Adaxial Segments

For the analysis of gene expression analysis, ChIP assay, western blot assay and confocal analysis, petioles were divided into abaxial and adaxial halves using razors. Samples were prepared on the basis of previous reports (Polko et al., 2013) with slight modifications.

Gene Expression Analysis

Transcript levels were analyzed by reverse transcription-mediated quantitative real-time PCR (RT-qPCR) according to the guidelines that have been proposed to assure reproducible and accurate measurements (Udvardi et al., 2008). RT-qPCR reactions were conducted in 384-well blocks with the Applied Biosystems QuantStudio 6 Flex (Foster City, CA) using the SYBR Green I master mix in a volume of 10 µl (Han et al., 2018). The two-step thermal cycling profile employed was 15 s at 95°C for denaturation and 1 min at 60–65°C, depending on the calculated melting temperatures of PCR primers, for annealing and polymerization. PCR primers used are listed in Table S1. The *eIF4A* gene (At3g13920) was included as internal control in PCR reactions to normalize the variations in the amounts of primary cDNAs used.

All RT-qPCR reactions were performed using three independent RNA samples, each of which was prepared from a pool of sixteen independent plant materials. The comparative $\Delta\Delta C_T$ method was employed to evaluate relative quantities of each amplified product in the samples. The threshold cycle (C_T) was automatically determined for each reaction by the system set with default parameters.

Confocal Microscopy

Transgenic plants expressing *PIN3* gene driven by the endogenous *PIN3* promoter have been frequently employed in confocal imaging assays on nastic and tropic responses, such as shade avoidance and hypocotyl phototropism and gravitropism (Keuskamp *et al.,* 2010; Ding *et al.,* 2011; Rakusová *et al.,* 2011).

Three-week-old p*PIN3:PIN3-GFP* transgenic plants were transferred to 28°C for 6 h. Following temperature treatments, the petioles of the 5th and 6th rosette leaves were dissected so that the longitudinal sections were placed on cover glasses. The dissected petiole samples

were subjected to fluorescence imaging using the SP8 X confocal microscope (Leica, Wetzlar, Germany).

It is known that chlorophyll autofluorescence is relatively weaker in endodermal cells than in epidermal cells (Keuskamp *et al.,* 2010). We visualized PIN3-GFP distribution in the endodermal cells of the petioles using a Leica SP8 X microscope with the following laser and filter setup: white light laser, 488 nm for excitation, 490 to 600 nm for emission to detect GFP, and 561 nm for excitation, 650 to 750 nm for emission to detect chlorophyll autofluorescence. The magnification value was set to 10. Fluorescence signals from 10 endodermal cells per sample were analyzed using the Leica Application Suite X (http://www.leica-microsystems.com/home/) and the ImageJ software. GFP and autofluorescence signals of outer membranes were quantified per 1500 μm^2 of samples.

To examine auxin accumulation, three-week-old DII-VENUS plants were temperature-treated, and epidermal regions were subjected to fluorescence imaging using an Olympus BX53 microscope with the following laser and filter setup: Olympus U-HGLGPS laser, 480 to 500 nm for excitation, 510 to 560 nm for emission to detect VENUS. The magnification value was set to 4. VENUS signals were counted per 2 mm^2 of sample area to quantify DII-VENUS fluorescence.

Pharmacological Treatment

For BFA treatments, a 10 μM BFA solution (Sigma-Aldrich, St. Louis, MO) was sprayed onto three-week-old plants prior to temperature treatments. For treatments with histone deacetylase inhibitors, 3 μM TSA (Sigma-Aldrich) and 30 μM CAY (Cayman Chemical, Ann Arbor, USA) solutions were sprayed onto three-week-old plants prior to temperature treatments. For treatments with auxin biosynthesis and transport inhibitors, 250 μM yucasin (Nishimura et al., 2014) and 10 μM NPA (Sigma-Aldrich) solutions were sprayed onto three-week-old plants before exposure to 28°C.

532

533 **ChIP**

534 ChIP assays were performed essentially as described previously (Lee et al., 2014). Briefly,
535 three-week-old plants grown on MS-agar plates were harvested at ZT24 and vacuum-
536 infiltrated with 1% (v/v) formaldehyde for cross-linking. The plant materials were then
537 ground in liquid nitrogen after quenching the cross-linking process and resuspended in 30 ml
538 of nuclear extraction buffer (1.7 M sucrose, 10 mM Tris-Cl, pH 7.5, 2 mM $MgCl_2$, 0.15%
539 (v/v) Triton-X-100, 5 mM β-mercaptoethanol, 0.1 mM PMSF) containing protease inhibitors
540 (Sigma-Aldrich) and filtered through miracloth filters (Millipore, Darmstadt, Germany). The
541 filtered mixture was centrifuged at 4,300 X g for 20 min at 4°C, and nuclear fractions were
542 isolated by the sucrose cushion method. The nuclear fractions were lysed with lysis buffer (50
543 mM Tris-Cl, pH 8.0, 0.5 M EDTA, 1% SDS) containing protease inhibitors and sonicated to
544 obtain chromatin fragments of 400–700 bps.

545 Five μg of anti-FLAG (Sigma-Aldrich) or anti-H4Ac (Millipore) antibody was added
546 to the chromatin solution and incubated for 16 h at 4°C. The Protein-G or Protein-A agarose
547 beads (Millipore) were then added to the solution and incubated for 1 h. The incubated
548 mixture was centrifuged at 4,000 X g for 2 min at 4°C. Following reverse crosslinking of the
549 precipitates, residual proteins were removed by treatments with proteinase K. DNA fragments
550 were purified using a silica membrane spin column (Promega, Madison, WI). To determine
551 the amounts of DNA enriched in chromatin preparations, quantitative PCR was performed,
552 and the values were normalized to the amount of input in each sample.

553

554 **Immunological Assay**

555 Plant materials were ground in liquid nitrogen. The ground plant materials were resuspended
556 in protein extraction buffer (100 mM Tris-Cl, pH 6.8, 4% SDS, 0.2% bromophenol blue, 20%
557 glycerol, and 200 mM β-mercaptoethanol). The mixtures were boiled for 10 min and then

centrifuged at 16,000 X g for 10 min at 4°C. The supernatants were analyzed by SDS-PAGE. The separated proteins were transferred to polyvinylidene difluoride membrane. Anti-H4Ac (Millipore), anti-tubulin (Sigma-Aldrich), and anti-H3 (Millipore) antibodies were used for the immunological detection of H4Ac, tubulin, and H3 proteins, respectively. Anti-rabbit and anti-mouse IgG-peroxidase antibodies (Santa Cruz Biotechnology, Santa Cruz, CA) were used as secondary antibodies for the immunoblot assays with anti-H4Ac, anti-H3 and anti-tubulin primary antibodies, respectively.

Statistical Analysis

The statistical significance between two means of measurements was determined using a two-sided Student's *t*-test with *P* values of < 0.01 or < 0.05. To determine statistical significance for more than two populations, one-way analysis of variance (ANOVA) with *post hoc* Tukey test ($P < 0.01$) was used. Statistical analyses were performed using the Rstudio software (https://www.rstudio.com/). Three independent measurements were statistically analyzed for phenotypic assays and gene expression analysis otherwise mentioned.

Accession Numbers

Sequence data from this article can be found in the GenBank/EMBL data libraries under accession numbers: *PIF4, AT2G43010; PID, AT2G34650; PIN3, AT1G70940; AS1, AT2G37630; SAUR19, AT5G18010; SAUR22, AT5G18050; TIR1, AT3G62980; AHA1, AT2G18960; AHA2, AT4G30190; PP2A, AT1G69960; D6PK, AT5G55910; WAG1, AT1G53700; WAG2, AT3G14370; YUC8, AT4G28720; eIF4A, AT3G13920.*

SUPPLEMENTAL DATA

Supplemental Figure S1. Auxin distribution in the abaxial and adaxial petiole regions during leaf thermonasty.

584 **Supplemental Figure S2.** Both auxin biosynthesis and its polar transport are involved in leaf
585 thermonasty.
586 **Supplemental Figure S3.** PIN3 is associated with leaf thermonasty.
587 **Supplemental Figure S4.** Thermo-induced polarization of PIN3 is mediated by vesicular
588 trafficking.
589 **Supplemental Figure S5.** PID is associated with leaf thermonasty.
590 **Supplemental Figure S6.** PIF4 mediates PIN3 polarization during leaf thermonasty.
591 **Supplemental Figure S7.** Thermonastic leaf movements in *as1-1* mutant.
592 **Supplemental Figure S8.** Thermo-induced PIN3 polarization is disrupted in *as1-1* mutant.
593 **Supplemental Figure S9.** H4 acetylation is related with leaf thermonasty.
594 **Supplemental Figure S10.** Transcription of *PIN3* and *PID* genes in different genetic
595 backgrounds.
596 **Supplemental Table S1.** Primers used in this work.
597

598 **ACKNOWLEDGMENTS**
599 We would like to thank Jae-Yean Kim for the DII-VENUS reporter plants. We also would like
600 to thank Tomokazu Koshiba for providing yucasin. The *pid wag1 wag2* mutant was obtained
601 from Remko Offringa.
602
603 **FIGURE LEGENDS**
604

605 **Figure 1.** Polarization of leaf thermonasty is independent of light direction and gravity.

606 Elevation angles of the 5th and 6th rosette leaves relative to the horizontal plane were
607 measured using three-week-old plants exposed to 28°C. Three independent measurements,
608 each consisting of 16 individual plants grown under identical conditions, were statistically

analyzed using Student's *t*-test (*$P < 0.01$, difference from 23°C). Error bars indicate standard error of the mean (SE). h, hour. A, Kinetic effects of warm temperatures on petiole bending. Elevation angles were measured in a time course following exposure to 28°C. B, Leaf petiole temperatures. Temperatures on the abaxial and adaxial surfaces of leaf petioles were measured by infrared thermography 6 h following exposure to 28°C. C, Effects of light direction on leaf thermonasty. Plants were exposed to 28°C for 6 h with upward light illumination. D, Kinetic effects of warm temperatures and light directions on petiole bending. Elevation angles were measured in a time course following exposure to 28°C with upward light illumination. E, Effects of gravity on leaf thermonasty. Plants were subjected to horizontal gravitropic stimulation (*g*) at 28°C for 6 h in the light. F, Kinetic effects of warm temperatures and gravity on petiole bending. Elevation angles were measured in a time course following exposure to 28°C with horizontal gravitropic stimulation, as depicted in (E).

Figure 2. Expression of auxin response genes is elevated in the abaxial petiole region during leaf thermonasty.

Three independent measurements, each consisting of 16 individual plants grown under identical conditions, were subjected to statistical analysis. Different letters represent a significant difference ($P < 0.01$) determined by one-way analysis of variance with *post hoc* Tukey test. Error bars indicate SE. A, Transcription of *SMALL AUXIN UP RNA* (*SAUR*) genes. Three-week-old Col-0 plants were exposed to 28°C before preparing dissected petiole samples for total RNA extraction. Transcript levels were analyzed by RT-qPCR. B, Leaf thermonasty in *tir1-1* mutant. Plants were temperature-treated as described above. C, Transcription of *glucuronidase* (*GUS*) reporter. The DR5:GUS plants were exposed to 28°C for 6 h, and petiole sampling and RT-qPCR were performed as described above. D, Leaf thermonasty in *pin3-4* mutant. Statistical analysis was performed using Student's *t*-test (*$P <$ 0.01, difference from 23°C). E, Transcription of *SAUR* genes in *pin3-4* and *pif4-101* mutants.

Temperature treatments, preparation of petiole samples, and RT-qPCR were performed as described above.

Figure 3. PIN3 is polarized to the outer membranes of abaxial endodermal cells in leaf petioles at warm temperatures.

Three independent measurements, each consisting of 8 individual plants grown under identical conditions, were statistically analyzed. Error bars indicate SE. In (C) and (D), different letters represent a significant difference ($P < 0.01$) determined by one-way analysis of variance with *post hoc* Tukey test. A and B, Polar distribution of PIN-FORMED 3 (PIN3). Three-week-old plants expressing a *PIN3-GFP* fusion driven by the endogenous *PIN3* promoter were exposed to 28°C for 6 h before fluorescence microscopy of the 5th leaf petioles. Green and red signals indicate PIN3-GFP and chlorophyll autofluorescence, respectively (A). Arrowheads indicate the outer membranes of petiole endodermal cells. Scale bars, 100 μm. PIN3-GFP signals were quantitated (*t*-test, $*P < 0.01$) (B). C, Effects of brefeldin A (BFA) on leaf thermonasty. A 10 μM BFA solution was sprayed on the petioles before exposure to 28°C. Elevation angles were measured and statistically analyzed. D, Transcription of *PINOID* (*PID*) gene. Leaf petioles of Col-0 plants were dissected into abaxial and adaxial halves. Transcript levels were analyzed by RT-qPCR.

Figure 4. PID-directed PIN3 polarization underlies leaf thermonasty.

Three independent measurements, each consisting of 16 individual plants grown under identical conditions, were statistically analyzed. In (C) and (D), different letters represent a significant difference ($P < 0.01$) determined by one-way analysis of variance with *post hoc* Tukey test. Error bars indicate SE. A and B, Polar distribution of PIN3. Three-week-old plants expressing a *PIN3-GFP* fusion driven by the endogenous *PIN3* promoter were exposed to

28°C for 6 h before fluorescence microscopy of the 5th leaf petioles (A). Arrowheads indicate the outer membranes of petiole endodermal cells. Scale bars, 100 μm. PIN3-GFP signals were quantitated (*t*-test, $*P < 0.01$) (B). (C) Leaf thermonasty in 35S:*PID* plants. (D) Transcription of *SAUR22* gene in 35S:*PID* plants. Leaf petioles were dissected into abaxial and adaxial halves. Transcript levels were analyzed by RT-qPCR.

Figure 5. PIF4 and AS1-mediated developmental signals activate *PID* transcription in the abaxial petiole region at warm temperatures.

Three independent measurements, each consisting of 16 individual plants grown under identical conditions, were statistically analyzed. Different letters represent a significant difference ($P < 0.01$) determined by one-way analysis of variance with *post hoc* Tukey test. Error bars indicate SE (A and D) or standard deviation of the mean (SD) (C, E, and F). A, *PID* transcription in *pif4-101* mutant. Three-week-old plants were exposed to 28°C for 6 h. Transcript levels were analyzed by RT-qPCR. B, Genomic structure of *PID* locus. Black boxes are exons, and white boxes are 5' and 3' untranslated regions. The P1 - P3 sequences were analyzed in chromatin immunoprecipitation (ChIP) assays. C, PHYTOCHROME INTERACTING FACTOR 4 (PIF4) binding to *PID* promoter. Three-week-old plants expressing a *PIF4-FLAG* fusion driven by the endogenous *PIF4* promoter were exposed to 28°C for 6 h. ChIP assays were performed using an anti-FLAG antibody. D, Transcription of *PID* gene in *as1-1* leaf petioles. Transcript levels were analyzed by RT-qPCR. E, PIF4 binding to *PID* promoter in *as1-1* mutant. A *PIF4-FLAG* fusion was expressed driven by the endogenous *PIF4* promoter in Col-0 plants and *as1-1* mutant. The P3 sequence was used in the assay. F, Histone 4 (H4) acetylation in *PID* chromatin. ChIP assays were performed using either Col-0 or *as1-1* leaf petioles. An anti-H4Ac antibody was used for immunoprecipitation.

682 H4 acetylation was analyzed by ChIP-qPCR. M, mock.

683

684 **Figure 6.** Leaf cooling is associated with hyponastic leaf movement. Three-week-old plants
685 were exposed to 28°C for 6 h before taking infrared thermographs (left panels). Elevation
686 angles were given below thermographs. Temperatures at the central blade areas of the 6th
687 rosette leaves were measured (right graphs). Three independent measurements, each
688 consisting of 8 individual plants grown under identical conditions, were statistically analyzed.
689 Different letters represent a significant difference ($P < 0.01$) determined by one-way analysis
690 of variance with *post hoc* Tukey test. Error bars indicate SE. A and B, Leaf temperatures in
691 *pif4-101* mutant. For comparison, the mutant rosette leaves were physically lifted to mimic
692 the increased leaf hyponasty as observed in Col-0 plants. C and D, Leaf temperatures in Col-0
693 plants having physically arrested leaf hyponasty. The rosette leaves were arrested physically
694 to the soil so that leaf hyponasty is not elevated at 28°C. Arrows marks arresting wires.

695

696 **Figure 7.** Schematic model for developmental shaping of polar auxin flow during leaf
697 thermonasty.
698 Thermo-activated PIF4 triggers auxin production in the leaf blade. Auxin is then transported
699 to the petiole, where it is distributed toward epidermis via PIN3. PIF4 also activates *PID*
700 transcription in the petiole. The leaf polarity determinant ASYMMETRIC LEAVES 1 (AS1)
701 directs *PID* transcription to occur predominantly in the abaxial petiole region. The PID-
702 mediated PIN3 polarization to the outer membrane of abaxial petiole cells determines the
703 direction of leaf bending. Blue arrows marks the paths of auxin flow.

704

705

Parsed Citations

Akhtar A, and Becker PB (2000) Activation of transcription through histone H4 acetylation by MOF, an acetyltransferase essential for dosage compensation in Drosophila. Mol Cell 5: 367-375

Pubmed: Author and Title
Google Scholar: Author Only Title Only Author and Title

Bai F, and Demason DA (2008) Hormone interactions and regulation of PsPK2::GUS compared with DR5::GUS and PID::GUS in Arabidopsis thaliana. Am J Bot 95: 133-145

Pubmed: Author and Title
Google Scholar: Author Only Title Only Author and Title

Crawford AJ, McLachlan DH, Hetherington AM, Franklin KA (2012) High temperature exposure increases plant cooling capacity. Curr Biol 22: R396-R397

Pubmed: Author and Title
Google Scholar: Author Only Title Only Author and Title

Dhonukshe P, Huang F, Galvan-Ampudia CS, Mähönen AP, Kleine-Vehn J, Xu J, Quint A, Prasad K, Friml J, Scheres B, et al (2010) Plasma membrane-bound AGC3 kinases phosphorylate PIN auxin carriers at TPRXS(N/S) motifs to direct apical PIN recycling. Development 137: 3245-3255

Pubmed: Author and Title
Google Scholar: Author Only Title Only Author and Title

Ding Z, Galván-Ampudia CS, Demarsy E, Łangowski Ł, Kleine-Vehn J, Fan Y, Morita MT, Tasaka M, Fankhauser C, Offringa R, et al (2011) Light-mediated polarization of the PIN3 auxin transporter for the phototropic response in Arabidopsis. Nat Cell Biol 13: 447-452

Pubmed: Author and Title
Google Scholar: Author Only Title Only Author and Title

Forterre Y, Skotheim JM, Dumais J, Mahadevan L (2005) How the Venus flytrap snaps. Nature 433: 421-425

Pubmed: Author and Title
Google Scholar: Author Only Title Only Author and Title

Franklin KA, Lee SH, Patel D, Kumar SV, Spartz AK, Gu C, Ye S, Yu P, Breen G, Cohen JD, et al (2011) Phytochrome-interacting factor 4 (PIF4) regulates auxin biosynthesis at high temperature. Proc Natl Acad Sci USA 108: 20231-20235

Pubmed: Author and Title
Google Scholar: Author Only Title Only Author and Title

Friml J, Wiśniewska J, Benková E, Mendgen K, Palme K (2002) Lateral relocation of auxin efflux regulator PIN3 mediates tropism in Arabidopsis. Nature 415: 806-809

Pubmed: Author and Title
Google Scholar: Author Only Title Only Author and Title

Ganguly A, Lee SH, Cho HT (2012) Functional identification of the phosphorylation sites of Arabidopsis PIN-FORMED 3 for its subcellular localization and biological role. Plant J 71: 810-823

Pubmed: Author and Title
Google Scholar: Author Only Title Only Author and Title

Gray WM, Ostin A, Sandberg G, Romano CP, Estelle M (1998) High temperature promotes auxin-mediated hypocotyl elongation in Arabidopsis. Proc Natl Acad Sci USA 95: 7197-7202

Pubmed: Author and Title
Google Scholar: Author Only Title Only Author and Title

Han SH, Park YJ, Park CM (2018) Light Primes the Thermally Induced Detoxification of Reactive Oxygen Species during Thermotolerance Development in Arabidopsis. Plant Cell Physiol doi: 10.1093/pcp/pcy206

Pubmed: Author and Title
Google Scholar: Author Only Title Only Author and Title

Huang CF, Yu CP, Wu YH, Lu MJ, Tu SL, Wu SH, Shiu SH, Ku MSB, Li WH (2017) Elevated auxin biosynthesis and transport underlie high vein density in C4 leaves. Proc Natl Acad Sci USA 114: E6884-6891

Pubmed: Author and Title
Google Scholar: Author Only Title Only Author and Title

Ibañez C, Delker C, Martinez C, Bürstenbinder K, Janitza P, Lippmann R, Ludwig W, Sun H, James GV, Klecker M, et al (2018) Brassinosteroids Dominate Hormonal Regulation of Plant Thermomorphogenesis via BZR1. Curr Biol 28: 303-310

Pubmed: Author and Title
Google Scholar: Author Only Title Only Author and Title

Iwasaki M, Takahashi H, Iwakawa H, Nakagawa A, Ishikawa T, Tanaka H, Matsumura Y, Pekker I, Eshed Y, Vial-Pradel S, et al (2013) Dual regulation of ETTIN (ARF3) gene expression by AS1-AS2, which maintains the DNA methylation level, is involved in stabilization of leaf adaxial-abaxial partitioning in Arabidopsis. Development 140: 1958-1969

Pubmed: Author and Title
Google Scholar: Author Only Title Only Author and Title

Izhaki A, Bowman JL (2007) KANADI and class III HD-Zip gene families regulate embryo patterning and modulate auxin flow during

embryogenesis in Arabidopsis. Plant Cell 19: 495-508
Pubmed: Author and Title
Google Scholar: Author Only Title Only Author and Title

Kerstetter RA, Bollman K, Taylor RA, Bomblies K, Poethig RS (2001) KANADI regulates organ polarity in Arabidopsis. Nature 411: 706-709
Pubmed: Author and Title
Google Scholar: Author Only Title Only Author and Title

Keuskamp DH, Pollmann S, Voesenek LA, Peeters AJ, Pierik R (2010) Auxin transport through PIN-FORMED 3 (PIN3) controls shade avoidance and fitness during competition. Proc Natl Acad Sci USA 107: 22740-22744
Pubmed: Author and Title
Google Scholar: Author Only Title Only Author and Title

Kleine-Vehn J, Huang F, Naramoto S, Zhang J, Michniewicz M, Offringa R, Friml J (2009) PIN auxin efflux carrier polarity is regulated by PINOID kinase-mediated recruitment into GNOM-independent trafficking in Arabidopsis. Plant Cell 21: 3839-3849
Pubmed: Author and Title
Google Scholar: Author Only Title Only Author and Title

Koini MA, Alvey L, Allen T, Tilley CA, Harberd NP, Whitelam GC, Franklin KA (2009) High temperature-mediated adaptations in plant architecture require the bHLH transcription factor PIF4. Curr Biol 19: 408-413
Pubmed: Author and Title
Google Scholar: Author Only Title Only Author and Title

Lippincott BB, Lippincott JA (1971) Auxin-induced hyponasty of the leaf blade of Phaseolus vulgaris. Amer J Bot 58: 817-826
Pubmed: Author and Title
Google Scholar: Author Only Title Only Author and Title

Lorrain S, Allen T, Duek PD, Whitelam GC, Fankhauser C (2008) Phytochrome-mediated inhibition of shade avoidance involves degradation of growth-promoting bHLH transcription factors. Plant J 53: 312-323
Pubmed: Author and Title
Google Scholar: Author Only Title Only Author and Title

Marhavý P, Vanstraelen M, De Rybel B, Zhaojun D, Bennett MJ, Beeckman T, Benková E (2013) Auxin reflux between the endodermis and pericycle promotes lateral root initiation. EMBO J 32: 149-158
Pubmed: Author and Title
Google Scholar: Author Only Title Only Author and Title

Merelo P, Ram H, Pia Caggiano M, Ohno C, Ott F, Straub D, Graeff M, Cho SK, Yang SW, Wenkel S, et al (2016) Regulation of MIR165/166 by class II and class III homeodomain leucine zipper proteins establishes leaf polarity. Proc Natl Acad Sci USA 113: 11973-11978
Pubmed: Author and Title
Google Scholar: Author Only Title Only Author and Title

Michaud O, Fiorucci AS, Xenarios I, Fankhauser C (2017) Local auxin production underlies a spatially restricted neighbor-detection response in Arabidopsis. Proc Natl Acad Sci USA 114: 7444-7449
Pubmed: Author and Title
Google Scholar: Author Only Title Only Author and Title

Nick P, Schafer E (1989) Nastic response of maize (Zea mays L.) coleoptiles during clinostat rotation. Planta 179: 123-131
Pubmed: Author and Title
Google Scholar: Author Only Title Only Author and Title

Nishimura T, Hayashi K, Suzuki H, Gyohda A, Takaoka C, Sakaguchi Y, Matsumoto S, Kasahara H, Sakai T, Kato J, et al (2014) Yucasin is a potent inhibitor of YUCCA, a key enzyme in auxin biosynthesis. Plant J 77: 352-366
Pubmed: Author and Title
Google Scholar: Author Only Title Only Author and Title

Lee H.J, Jung JH, Cortés Llorca L, Kim SG, Lee S, Baldwin IT, Park CM (2014) FCA mediates thermal adaptation of stem growth by attenuating auxin action in Arabidopsis. Nat. Commun 5: 5473
Pubmed: Author and Title
Google Scholar: Author Only Title Only Author and Title

Oh E, Zhu JY, Wang ZY (2012) Interaction between BZR1 and PIF4 integrates brassinosteroid and environmental responses. Nat Cell Biol 14: 802-809
Pubmed: Author and Title
Google Scholar: Author Only Title Only Author and Title

Pantazopoulou CK, Bongers FJ, Küpers JJ, Reinen E, Das D, Evers JB, Anten NPR, Pierik R (2017) Neighbor detection at the leaf tip adaptively regulates upward leaf movement through spatial auxin dynamics. Proc Natl Acad Sci USA 114: 7450-7455
Pubmed: Author and Title
Google Scholar: Author Only Title Only Author and Title

Park YJ, Lee HJ, Ha JH, Kim JY, Park CM (2017) COP1 conveys warm temperature information to hypocotyl thermomorphogenesis. New Phytol 215: 169-280
Pubmed: Author and Title
Google Scholar: Author Only Title Only Author and Title

Pubmed: Author and Title
Google Scholar: Author Only Title Only Author and Title

Pérez-Pérez JM, Candela H, Robles P, López-Torrejón G, del Pozo JC, Micol JL (2010) A role for AUXIN RESISTANT3 in the coordination of leaf growth. Plant Cell Physiol. 51: 1661-1673
Pubmed: Author and Title
Google Scholar: Author Only Title Only Author and Title

Petrásek J and Friml J (2009) Auxin transport routes in plant development. Development 136: 2675-2688
Pubmed: Author and Title
Google Scholar: Author Only Title Only Author and Title

Polko JK, Pierik R, van Zanten M, Tarkowská D, Strnad M, Voesenek LA, Peeters AJ (2013) Ethylene promotes hyponastic growth through interaction with ROTUNDIFOLIA3/CYP90C1 in Arabidopsis. J Exp Bot 64: 613-624
Pubmed: Author and Title
Google Scholar: Author Only Title Only Author and Title

Polko JK, Voesenek LA, Peeters AJ, Pierik R (2011) Petiole hyponasty: an ethylene-driven, adaptive response to changes in the environment. AoB Plants plr031
Pubmed: Author and Title
Google Scholar: Author Only Title Only Author and Title

Rahman A, Takahashi M, Shibasaki K, Wu S, Inaba T, Tsurumi S, Baskin TI (2010) Gravitropism of Arabidopsis thaliana roots requires the polarization of PIN2 toward the root tip in meristematic cortical cells. Plant Cell 22: 1762-1767
Pubmed: Author and Title
Google Scholar: Author Only Title Only Author and Title

Rakusová H, Gallego-Bartolomé J, Vanstraelen M, Robert HS, Alabadí D, Blázquez MA, Benková E, Friml J (2011) Polarization of PIN3-dependent auxin transport for hypocotyl gravitropic response in Arabidopsis thaliana. Plant J 67: 817-826
Pubmed: Author and Title
Google Scholar: Author Only Title Only Author and Title

Ryu H, Kim K, Cho H, Park J, Choe S, Hwang I (2007) Nucleocytoplasmic shuttling of BZR1 mediated by phosphorylation is essential in Arabidopsis brassinosteroid signaling. Plant Cell 19: 2749-2762
Pubmed: Author and Title
Google Scholar: Author Only Title Only Author and Title

Sasidharan R, Voesenek LA (2015) Ethylene-mediated acclimations to flooding stress. Plant Physiol 169: 3-12
Pubmed: Author and Title
Google Scholar: Author Only Title Only Author and Title

Sun J, Qi L, Li Y, Chu J, Li C (2012) PIF4-mediated activation of YUCCA8 expression integrates temperature into the auxin pathway in regulating Arabidopsis hypocotyl growth. PLoS Genet 8: e1002594
Pubmed: Author and Title
Google Scholar: Author Only Title Only Author and Title

Udvardi MK, Czechowski T, Scheible WR (2008) Eleven golden rules of quantitative RT-PCR. Plant Cell 20: 1736–1737
Pubmed: Author and Title
Google Scholar: Author Only Title Only Author and Title

Ueno Y, Ishikawa T, Watanabe K, Terakura S, Iwakawa H, Okada K, Machida C, Machida Y (2007) Histone deacetylases and ASYMMETRIC LEAVES2 are involved in the establishment of polarity in leaves of Arabidopsis. Plant Cell 19: 445-457
Pubmed: Author and Title
Google Scholar: Author Only Title Only Author and Title

van Zanten M, Voesenek LA, Peeters AJ, Millenaar FF (2009) Hormone- and light-mediated regulation of heat-induced differential petiole growth in Arabidopsis. Plant Physiol 151: 1446-1458
Pubmed: Author and Title
Google Scholar: Author Only Title Only Author and Title

Wang HZ, Yang KZ, Zou JJ, Zhu LL, Xie ZD, Morita MT, Tasaka M, Friml J, Grotewold E, Beeckman T, et al (2015) Transcriptional regulation of PIN genes by FOUR LIPS and MYB88 during Arabidopsis root gravitropism. Nat Commun 6: 8822
Pubmed: Author and Title
Google Scholar: Author Only Title Only Author and Title

Willige BC, Isono E, Richter R, Zourelidou M, Schwechheimer C (2011) Gibberellin regulates PIN-FORMED abundance and is required for auxin transport-dependent growth and development in Arabidopsis thaliana. Plant Cell 23: 2184-2195
Pubmed: Author and Title
Google Scholar: Author Only Title Only Author and Title

Weller B, Zourelidou M, Frank L, Barbosa IC, Fastner A, Richter S, Jürgens G, Hammes UZ, Schwechheimer C (2017) Dynamic PIN-FORMED auxin efflux carrier phosphorylation at the plasma membrane controls auxin efflux-dependent growth. Proc Natl Acad Sci USA 114: E887-E896
Pubmed: Author and Title
Google Scholar: Author Only Title Only Author and Title

Zádníková P, Petrásek J, Marhavy P, Raz V, Vandenbussche F, Ding Z, Schwarzerová K, Morita MT, Tasaka M, Hejátko J, et al (2010) Role of PIN-mediated auxin efflux in apical hook development of Arabidopsis thaliana. Development 137: 607-617
Pubmed: Author and Title
Google Scholar: Author Only Title Only Author and Title

Zhao Y (2010) Auxin biosynthesis and its role in plant development. Annu Rev Plant Biol 61: 49-64
Pubmed: Author and Title
Google Scholar: Author Only Title Only Author and Title

Zourelidou M, Absmanner B, Weller B, Barbosa IC, Willige BC, Fastner A, Streit V, Port SA, Colcombet J, de la Fuente van Bentem S, et al (2014) Auxin efflux by PIN-FORMED proteins is activated by two different protein kinases, D6 PROTEIN KINASE and PINOID. Elife 3: e02860
Pubmed: Author and Title
Google Scholar: Author Only Title Only Author and Title

Zgurski JM, Sharma R, Bolokoski DA, Schultz EA (2005) Asymmetric auxin response precedes asymmetric growth and differentiation of asymmetric leaf 1 and asymmetric leaf 2 Arabidopsis leaves. Plant Cell 17: 77-91
Pubmed: Author and Title
Google Scholar: Author Only Title Only Author and Title

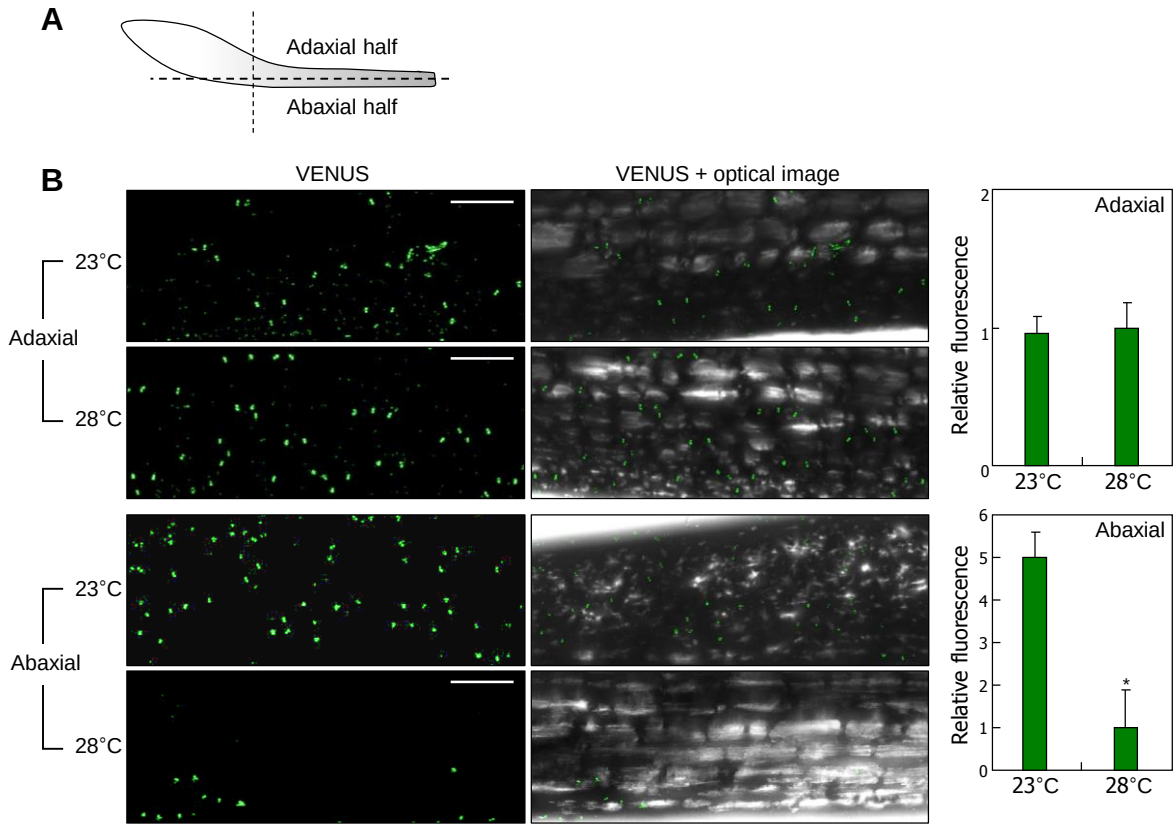

Supplemental Figure S1. Auxin distribution in the abaxial and adaxial petiole regions during leaf thermonasty. A, Schematic drawing of leaf petiole regions. B, Fluorescence imaging of abaxial and adaxial petiole regions in DII-VENUS reporter plants. Three-week-old transgenic plants expressing DII-VENUS were exposed to 28˚C for 6 h prior to fluorescence microscopy. Fluorescence images of the abaxial and adaxial epidermal petiole regions were obtained (left panels). Scale bars, 500 μm. Three independent measurements, each consisting of 8 individual plants grown under identical conditions, were statistically analyzed (*t*-test, $*P < 0.01$, difference from 23˚C) (right graphs). Error bars indicate standard error of the mean (SE).

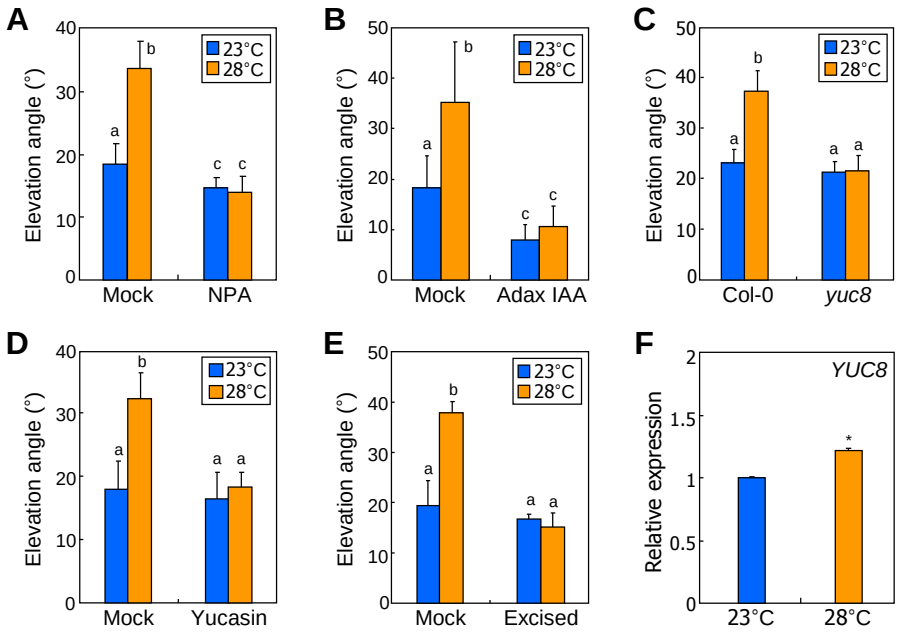

Supplemental Figure S2. Both auxin biosynthesis and its polar transport are involved in leaf thermonasty. Three-week-old Col-0 plants were exposed to 28˚C for 6 h. Three independent measurements, each consisting of 16 individual plants grown under identical conditions, were statistically analyzed. Different letters represent a significant difference ($P < 0.01$) determined by one-way analysis of variance (ANOVA) with *post hoc* Tukey test. Error bars indicate SE. A, Effects of 1-N-Naphthylphthalamic acid (NPA) on leaf thermonasty. Plants were sprayed with a 10 μM NPA solution, a specific inhibitor of auxin efflux, before warm temperature treatments. B, Localized application of IAA to the adaxial petiole region. Two μL of a 10 μM IAA solution was applied to the adaxial petiole region before warm temperature treatments. C, Leaf thermonasty in *yuc8* mutant. D, Effects of yucasin on leaf thermonasty. Plants were sprayed with a 250 μM yucasin solution before warm temperature treatments. Yucasin is a potent inhibitor of YUCCA, a key enzyme in auxin biosynthesis. E, Leaf thermonasty after excision of leaf blades. The leaf blades were excised before warm temperature treatments. F, *YUC8* transcription in the petioles. Three-week-old Col-0 plants were exposed to 28˚C for 6 h before harvesting leaf petioles for total RNA extraction. Transcript levels were analyzed by reverse transcription-mediated quantitative PCR (RT-qPCR). Statistical analysis was performed using Student's *t*-test (*$P < 0.01$).

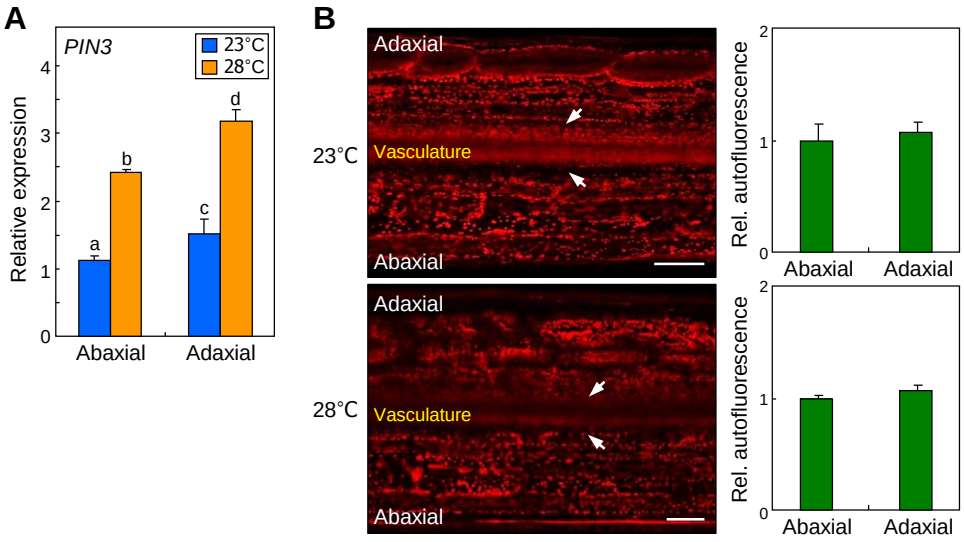

Supplemental Figure S3. PIN3 is associated with leaf thermonasty. A, PIN3 transcription in leaf petioles at 28˚C. Three-week-old Col-0 plants were exposed to 28˚C for 6 h before leaf petiole dissection and total RNA extraction for RT-qPCR. Three independent measurements, each consisting of 16 individual plants grown under identical conditions, were statistically analyzed. Different letters represent a significant difference ($P < 0.01$) determined by one-way ANOVA with *post hoc* Tukey test. Error bars indicate SE. B, Autofluorescence images of the petiole samples described in Figure 3a. White arrows indicate endodermal cells that were subjected to the measurements of fluorescence intensities (left panels). Scale bars, 100 μm. Autofluorescence intensities were measured using the LAS X software (Leica Microsystems, Wetzlar, Germany). Three independent measurements, each consisting of 8 individual plants grown under identical conditions, were statistically analyzed using Student's *t*-test (right graphs). Error bars indicate SE.

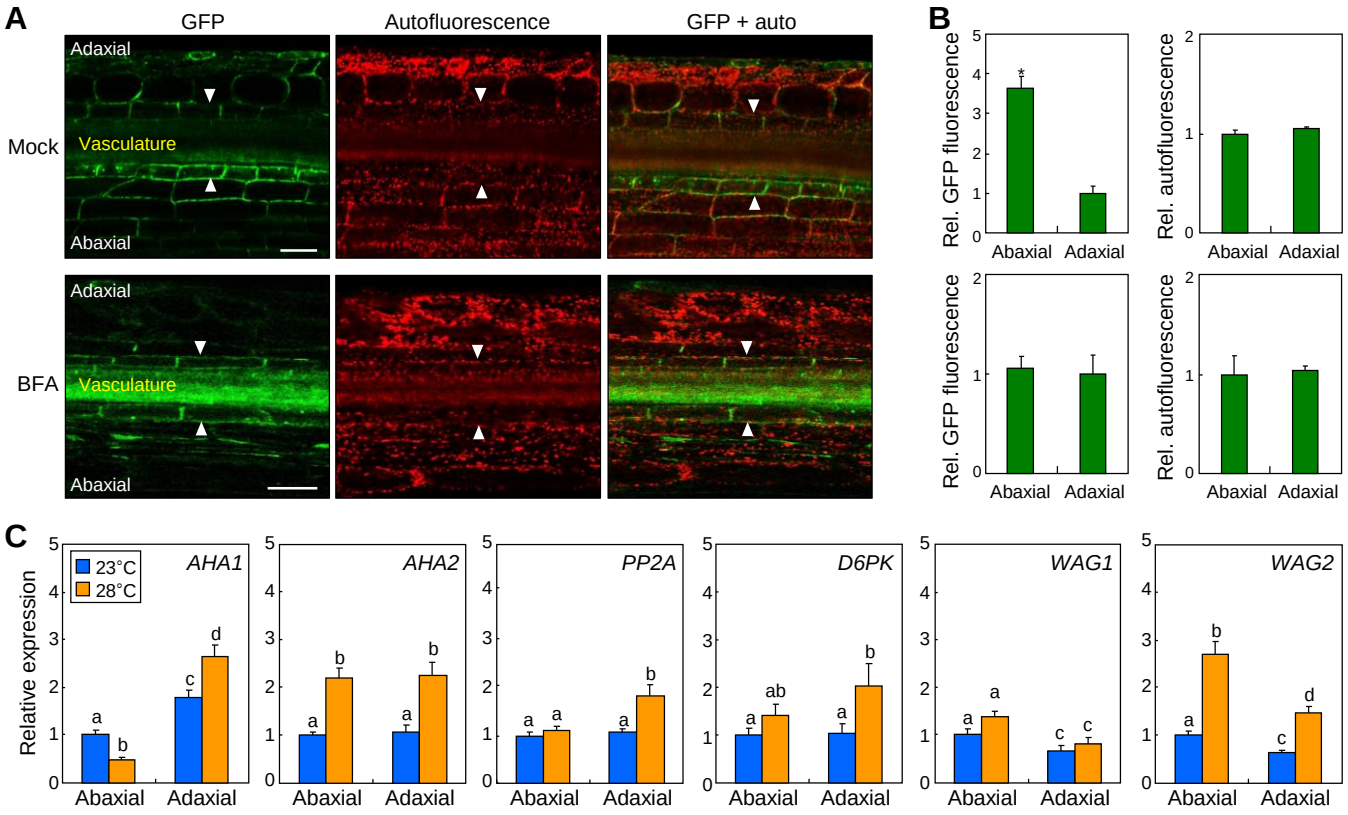

Supplemental Figure S4. Thermo-induced polarization of PIN3 is mediated by vesicular trafficking. A and B, Inhibition of polar PIN3 trafficking by brefeldin A (BFA). Three-week-old plants expressing a *PIN3-GFP* fusion driven by the endogenous *PIN3* promoter were sprayed with a 10 μM BFA solution before exposure to 28˚C for 6 h. BFA is a potent inhibitor of vesicular trafficking. Fluorescence images of the 5th leaf petioles were obtained (A). White arrowheads indicate the outer membranes of petiole endodermal cells. Scale bars, 100 μm. Relative GFP intensities in the outer membranes of adaxial and abaxial petiole cells were quantitated using the LAS X software (B). Relative autofluorescence intensities were also quantitated. Three independent measurements, each consisting of 8 individual plants grown under identical conditions, were statistically analyzed (*t*-test, $*P < 0.01$). Error bars indicate SE. C, Transcription of genes involved in PIN3 polarization. Three-week-old Col-0 plants were exposed to 28˚C for 6 h before leaf petiole dissection and total RNA extraction for RT-qPCR. Three independent measurements, each consisting of 16 individual plants grown under identical conditions, were statistically analyzed. Different letters represent a significant difference ($P < 0.01$) determined by one-way ANOVA with *post hoc* Tukey test. Error bars indicate SE. Genes examined include those encoding H^+-ATPase 1 (AHA1, AT2G18960), AHA2 (AT4G30190), serine/threonine protein phosphatase 2A (PP2A, AT1G69960), D6 protein kinase (D6PK, AT5G55910), WAG1 (AT1G53700), and WAG2 (AT3G14370).

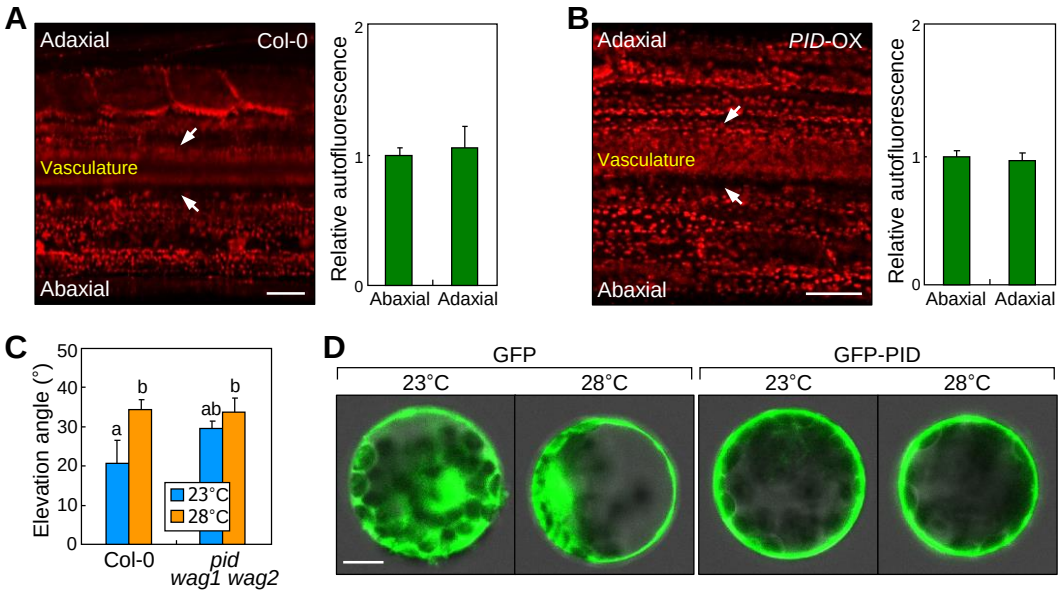

Supplemental Figure S5. PID is associated with leaf thermonasty. Three independent measurements, each consisting of 8 individual plants grown under identical conditions, were statistically analyzed. Error bars indicate SE. A and B, Autofluorescence images of the petiole samples described in Fig. 4A. Autofluorescence intensities were measured as described in Supplemental Fig. S3. Arrows indicate endodermal cells that were subjected to the measurements of fluorescence intensities. Scale bars, 100 μm. Statistical analysis was performed using Student's *t*-test (*$P < 0.01$). C, leaf thermonasty in *pid wag1 wag2* mutant. Warm temperature treatments and measurements of elevation angles were performed as described in Supplemental Fig. S2. Different letters represent a significant difference ($P < 0.01$) determined by one-way ANOVA with *post hoc* Tukey test. D, PID localization in *Arabidopsis* protoplasts. The 35S:*GFP-PID* gene expression fusion was transiently expressed in *Arabidopsis* protoplasts at either 23˚C or 28˚C for 6 h. The protoplasts were then subjected to confocal image analysis. Scale bar, 10 μm.

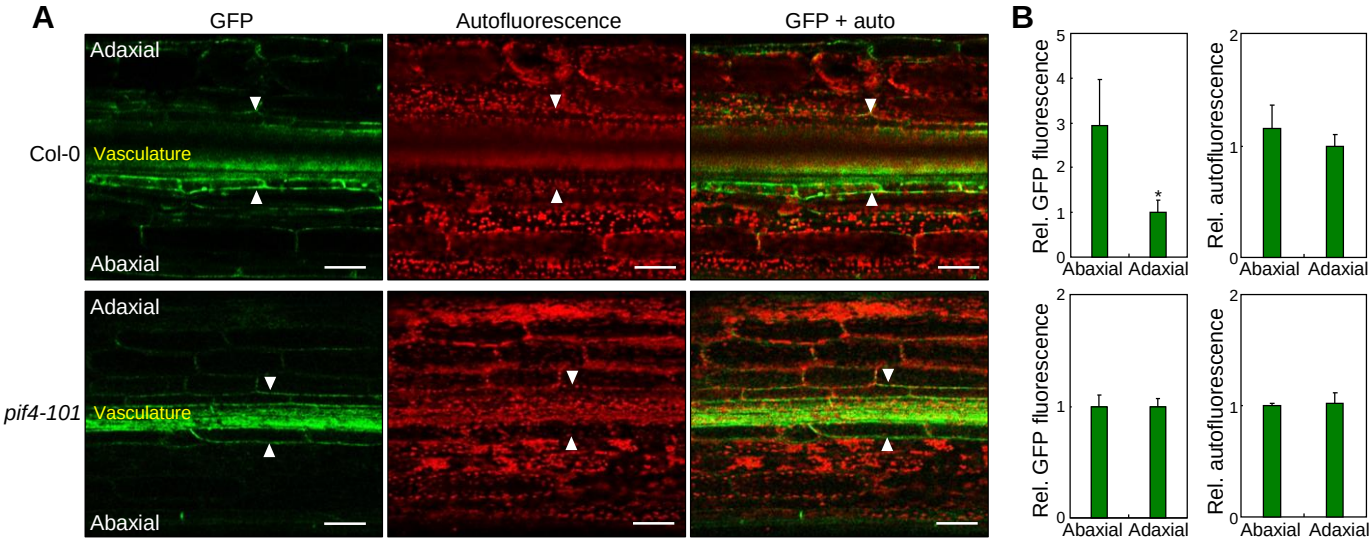

Supplemental Figure S6. PIF4 mediates PIN3 polarization during leaf thermonasty. A and B, Disruption of PIN3 polarization in *pif4-101* mutant. Warm temperature treatments and fluorescence microscopy were performed as described in Supplemental Fig. S3. Arrowheads indicate the outer membranes of endodermal petiole cells. Scale bars, 100 μm. Three independent measurements, each consisting of 16 individual plants grown under identical conditions, were statistically analyzed (*t*-test, $*P < 0.01$) (B). Error bars indicate SE.

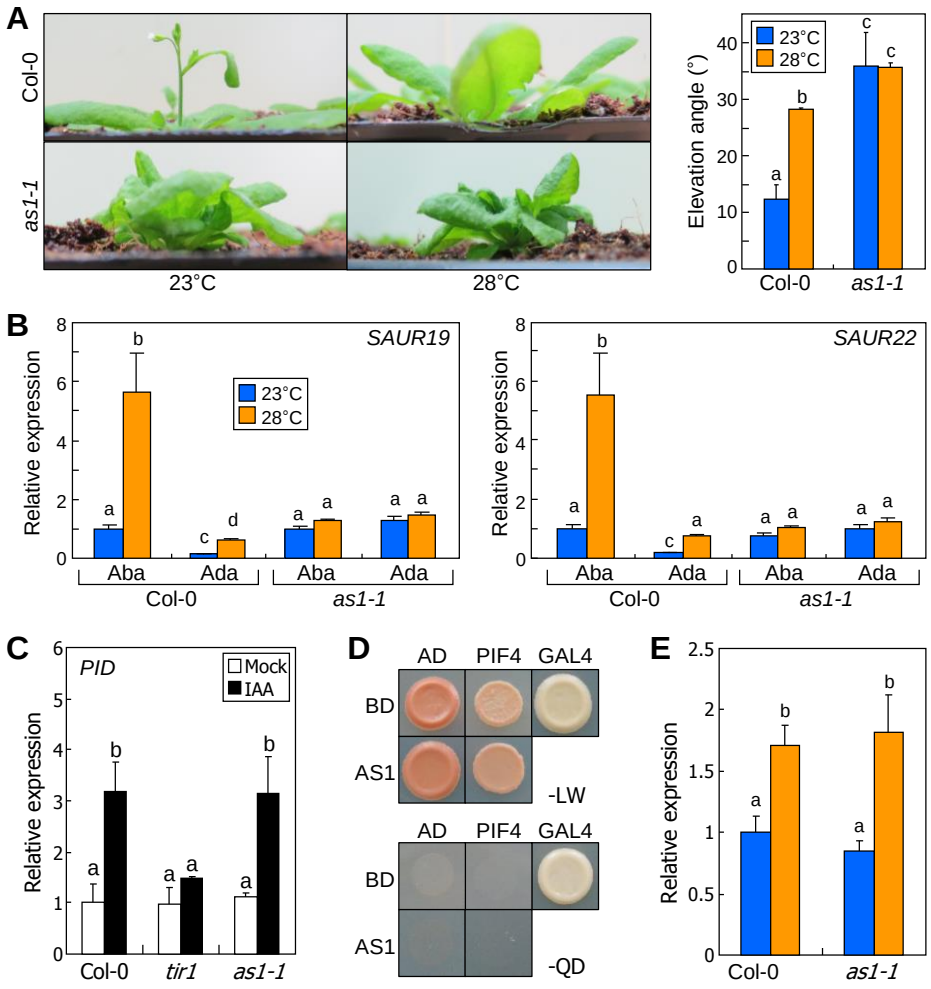

Supplemental Figure S7. Thermonastic leaf movements in *as1-1* mutant. Three independent measurements, each consisting of 16 individual plants grown under identical conditions, were statistically analyzed. Different letters represent a significant difference ($P < 0.01$) determined by one-way ANOVA with *post hoc* Tukey test (A and E). Error bars indicate SE. A, Leaf thermonasty in *as1-1* mutant. Warm temperature treatments and measurements of elevation angles were performed as described in Supplemental Fig. S2. B, Transcription of *SAUR* genes in *as1-1* leaf petioles. Preparation of leaf petiole samples and RT-qPCR were performed as described in Supplemental Fig. S3. C, IAA-mediated induction of *PID* transcription in *as1-1* mutant. Leaf petioles of three-week-old plants were treated with 10 μM IAA for 6 h. Transcript levels were analyzed by RT-qPCR. D, AS1 does not directly interact with PIF4. Yeast two-hybrid assays were employed to examine protein-protein interactions. -LW indicates Leu and Trp dropout plates. -QD indicates Leu, Trp, His, and Ade dropout plates. Yeast cells coexpressing AD and BD survive on –LW plates. Protein-protein interactions were confirmed by survival of yeast cells on -QD plates. Thirty mM of 3-amino-1,2,4-triazole (3-AT) was included in the growth media to inhibit autoactivity. E, *PIF4* transcription in *as1-1* mutant. Three-week-old plants were exposed to 28˚C for 6 h. Leaf petioles were harvested for total RNA extraction and RT-qPCR.

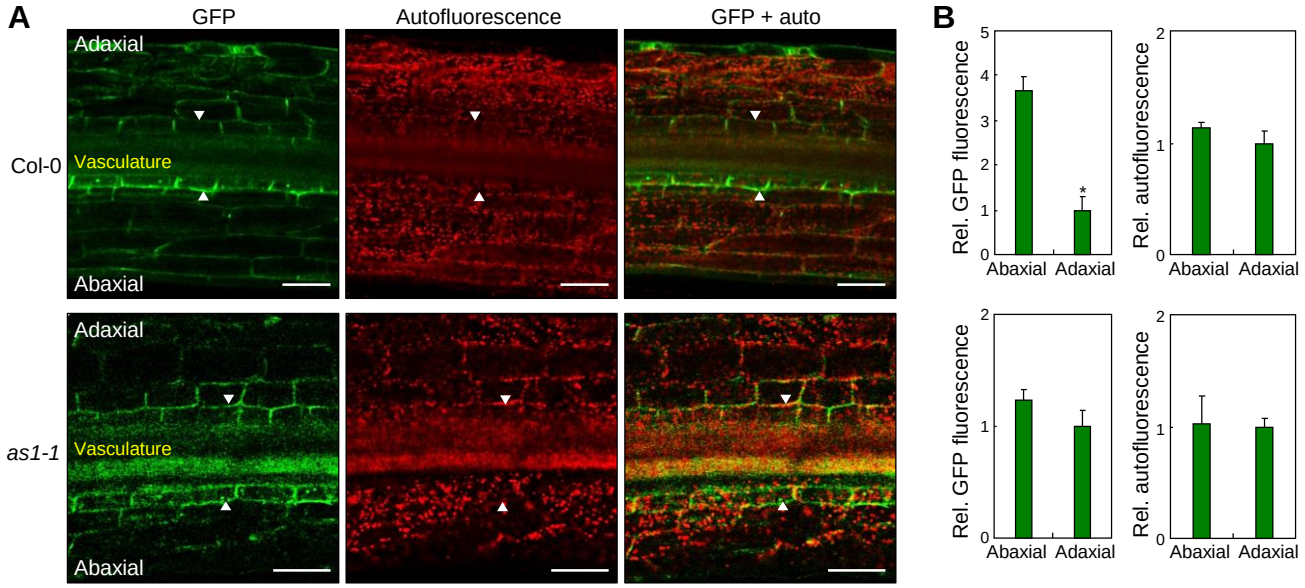

Supplemental Figure S8. Thermo-induced PIN3 polarization is disrupted in *as1-1* mutant. A and B, Disruption of PIN3 polarization in *as1-1* mutant. A *PIN3-GFP* fusion was expressed driven by the endogenous *PIN3* promoter in Col-0 plants and *as1-1* mutant. Warm temperature treatments and fluorescence microscopy were performed as described in Supplemental Fig. S3. Arrowheads indicate the outer membranes of endodermal petiole cells (A). Scale bars, 100 μm. Three independent measurements, each consisting of 8 individual plants grown under identical conditions, were statistically analyzed (*t*-test, $*P < 0.01$) (B). Error bars indicate SE.

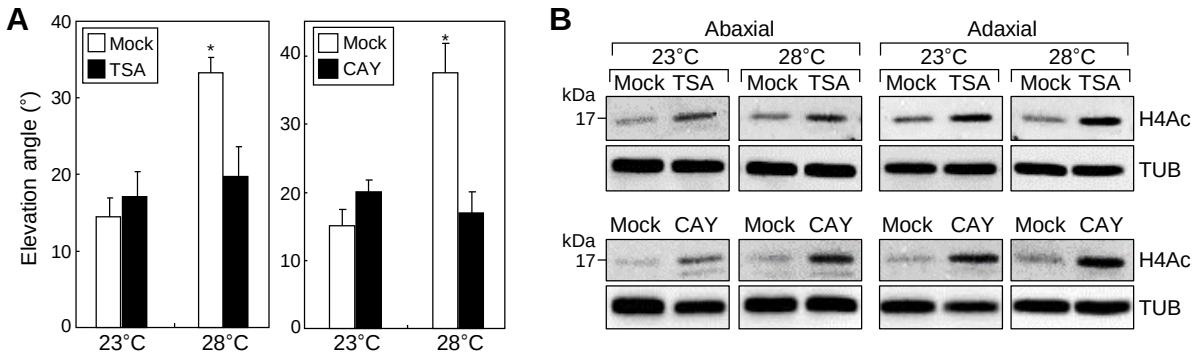

Supplemental Figure S9. H4 acetylation is related with leaf thermonasty. A and B, Effects of histone deacetylation inhibitors on leaf thermonasty. Three-week-old Col-0 plants were exposed to 28˚C for 6 h. Trichostatin A (TSA) and 4-(dimethylamino)-N-[6-(hydroxyamino)-6-oxohexyl]-benzamide (CAY) were used at concentrations of 3 μM and 30 μM, respectively. Three independent measurements, each consisting of 8 individual plants grown under identical conditions, were statistically analyzed (*t*-test, **P* < 0.01) (A). Error bars indicate SE. An anti-H4Ac antibody was used for the immunological verification of TSA and CAY treatments (B). Immunological detection of tubulin (TUB) was performed as loading control. kDa, kilodalton.

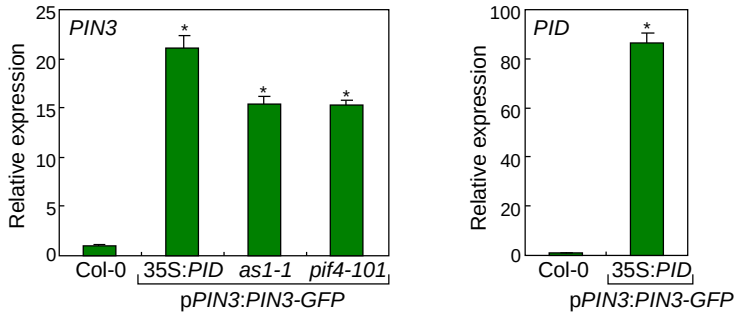

Supplemental Figure S10. Transcription of *PIN3* and *PID* genes in different genetic backgrounds. The p*PIN3*:*PIN3-GFP* expression fusion was transformed into different genetic backgrounds. The resultant transgenic plants were grown on MS-agar plates for ten days at 23˚C. Whole plants were harvested for total RNA extraction. RT-qPCR was performed as described in Fig. 2. Three independent measurements, each consisting of 16 individual plants grown under identical conditions, were statistically analyzed (*t*-test, **P* < 0.01, difference from Col-0). Error bars indicate SE.

Primers	Sequences	Usage
eIF4A-F	5′-TGACCACACAGTCTCTGCAA	RT-qPCR
eIF4A-R	5′-ACCAGGGAGACTTGTTGGAC	"
SAUR19-F	5'-CTTCAAGAGCTTCATAATAATTCAAACTT	"
SAUR19-R	5'-GAAGGAAAAAATGTTGGATCATCTT	"
SAUR22-F	5′-GACAAATAGAGAATTATAAATGGCTCTG	"
SAUR22-R	5′-ATGAATTAAGTCTATATCTAACTCGGAAA	"
PIN3-F	5′-CCAAATCGTCGTCCTCCAGT	"
PIN3-R	5′-TCCCGTCGTCACCTATCTCT	"
AHA1-F	5′-TCTCATGGCCATTGCTTTGG	"
AHA1-R	5′-GCATTTCCGGCGTTGTTTTC	"
AHA2-F	5′-CCCCCAAGACATGACAGTGC	"
AHA2-R	5′-AATGGATGCGAGGTTTGCGT	"
PP2A-F	5′-CGTGGTGCAGGCTACACTTT	"
PP2A-R	5′-ATGTTGCCACAACGGTAGCA	"
D6PK-F	5′-CTGCTTTGGCTAGCCGGAAA	"
D6PK-R	5′-CGTTTCCCGGGTTGTCTCTG	"
WAG1-F	5′-GCACGCTCAAGCCTAACCTT	"
WAG1-R	5′-CCGTCGGAGGAGAGAGTTGT	"
WAG2-F	5′-TCCACCACTACCGACCGTAC	"
WAG2-R	5′-AGGATCATGACGACGGTGGT	"
GUS-F	5′-GAATTGATCAGCGTTGGTGG	"
GUS-R	5′-ATCGAAACGCAGCACGATAC	"
PID-F	5′-TTCGCCGGAGAATCAACAAC	"
PID-R	5′-ACCGGTTCAGCAACAAAGAG	"
PID-P1-F	5′-GCACCCCTATAATATGCCTAGAGGA	ChIP-PCR
PID-P1-R	5′-TGCACTTTTCAACGCGTGAG	"
PID-P2-F	5′-AAACGGATTGAATCATCATTTAGCTT	"
PID-P2-R	5′-ACATCGGAATGACTTACTTCTGTGT	"
PID-P3-F	5′-CTCTTGCCAAAGTCCAGAAATATGAC	"
PID-P3-R	5′-AAAAGTCTCGACCCATATCACGA	"

Supplemental Table S1. Primers used in this work. The primers used were designed using the Primer3 software (version 0.4.0) available at http://primer3.sourceforge.net/releases.php in a way that they have calculated melting temperatures in a range of 50 - 60°C. F, forward primer; R, reverse primer.